LLNL-TR-805304

H2OI95: A Stand-Alone Fortran Code for Evaluating the IAPWS-95 Equation-of-State Model for Water (Rev. 1)

Thomas J. Wolery
Akima Infrastructure Services LLC
Lawrence Livermore National Laboratory

May 18, 2020

Contents

This report describes H2OI95, Version 1.1, Build 118. Errors in Version 1.1 that have been corrected are summarized in the Prologue. One specific error is noted in detail in Appendix C. Additional water properties calculated by Version 1.1 are described in Section 5. New Section 4.3 gives more information on the software verification of the implementation of the IAPWS-95 model.

Prologue

H2OI95 is a stand-alone Fortran code for evaluating the IAPWS-95 equation-of-state model (Wagner and Pruss, 2002; IAPWS, 2016) for the thermodynamic properties of water. Version 1.0 also evaluated the corresponding thermochemical properties of water consistent with the CODATA recommendations (Cox et al., 1989). Version 1.1 adds additional property calculations based on IAPWS-95 itself and through inclusion of associated models sanctioned by IAPWS. Additional properties derivable only from IAPWS-95 include the isobaric thermal expansivity and the isothermal compressibility. The isothermal compressibility had been a late addition to version 1.0 and appeared on the mtab.csv output file. The units given were MPa^{-1} (intended), but the values given were actually in kPa^{-1}. These and other additional properties are now on a new output file called xtab.csv, and isothermal compressibility values are now correctly given in MPa^{-1}. During testing of implementation of the viscosity model, an error was noted in the evaluation of the dimensionless isothermal compressibility as calculated from IAPWS-95. This error is discussed in Appendix C. It noticeably affects the calculation of some "higher-order" properties near the critical point. These properties include the isothermal compressibility and the isobaric heat capacity. Version 1.0 passed a number of verification tests without exposing this error. Parameters now included on the xtab.csv output file include the compressibility and thermal expansivity as noted above and the dynamic viscosity, thermal conductivity, surface tension, static dielectric constant, and the more significant of the various Debye-Hückel parameters. A future version of this software might include more Debye-Hückel parameters as well as various Born functions (for a description of such parameters, see Helgeson and Kirkham, 1974b). This might benefit from a better model for the dielectric constant than the one used here. Sections 1-4 of this manual have been updated for consistency with version 1.1. In most instances, there are no significant changes. Recalculation of the figures in these sections resulted in no noticeable changes. Where a notable change has occurred, it is called out in an 'UPDATE" included in the text. Some parts of the text have been updated for clarity or to discuss additional references. A new Section 4.3 has been added to summarize verification of the implementation of the IAPWS-95 model.

Abstract

H2OI95 is a stand-alone Fortran code for evaluating the IAPWS-95 equation-of-state model (Wagner and Pruss, 2002; IAPWS, 2016) for the thermodynamic properties of water. It also evaluates the corresponding thermochemical properties of water consistent with the CODATA recommendations (Cox et al., 1989). The IAPWS-95 model is based on a model equation for the dimensionless Helmholtz energy for which the primary variables are the *inverse* reduced temperature ($\tau = T_{cr}/T$) and reduced density ($\delta = \rho/\rho_{cr}$). Here T is the absolute temperature (K), ρ is density (kg/m^3), and the subscript "cr" refers to the critical point of water (647.096 K and 22.064 MPa pressure in this model, for which ρ_{cr} is 322 kg/m^3). The code solves four basic types of problems, distinguished by the specified inputs:

1, Temperature (K) and density (ρ kg/m^3) or reduced density (δ)

2. Temperature (K) and pressure (MPa).

3. Temperature (K) on the saturation (liquid-vapor equilibrium) curve

4. Pressure (MPa) on the saturation curve

Each type of problem is run using a corresponding input (text) file. All but the first type of problem require iteration. For example, to solve for desired temperature and pressure, the reduced density must be adjusted to give the desired pressure. Iteration is accomplished using the Newton-Raphson method, though the secant method is also used in solving the fourth type of problem. For the last three types of problems, H2OI95 has been used to conduct numerical studies of convergence and the problem of multiple numerical solutions, some of which are not physically valid. Obtaining valid results depends mainly on appropriate choice of starting values for the density. The default values used in H2OI95 appear to consistently lead to generally desired results. With modification (not addressed here), H2OI95 can be used to support SUPCRT92 (Johnson et al., 1992) and similar codes that compute chemical thermodynamic properties of species and reactions over a wide range of temperature and pressure (273.16-1273K and 0-1000 MPa). Version 1.1 of this software calculates an extended set of water properties, including some derivable solely from IAPWS-95, such as the isobaric thermal expansivity and the isothermal compressibility, and still other properties based on supplementary models sanctioned by IAPWS, including the dynamic viscosity, thermal conductivity, surface tension, and static dielectric constant, and various other properties (notably Debye-Hückel parameters) derivable from the dielectric constant and its partial derivatives with respect to temperature and pressure. A coding error in Version 1.0 was identified while testing the implementation of the viscosity model. This error is described in Appendix C. It mainly affects calculation of "higher order" properties such as compressibility and heat capacity near the critical point.

This page left blank.

1. Introduction

H2OI95 was written primarily to make the IAPWS-95 model (Wagner and Pruss, 2002; IAPWS, 2016) available in the program SUPCRT92 (Johnson et al., 1992) and other codes that similarly compute chemical thermodynamic properties of species and reactions at various temperatures and pressures. As presented here, H2OI95 is a stand-alone code. SUPCRT92 (unmodified) uses a combination of two older equation-of-state models, IAPS-84 (Haar et al., 1984) and, near the critical point, the model of Levelt Sengers et al. (1983). IAPWS-95 is recognized by the International Association for the Properties of Water and Steam (IAPWS) as the current standard model, IAPS-84 being the earlier standard. A still earlier standard equation-of-state model (Keenan et al., 1969) that did not extend to the critical point was used in the original SUPCRT program written in 1974-975 (see Johnson et al., 1992). That appears to have represented the first use of an equation-of-state model to calculate the thermochemical properties of water over a wide range of temperature and pressure. The IAPWS-95 model covers a temperature range of 273.16K (the triple point temperature) to 1273K, and a pressure range of 0-1000 MPa. This includes the critical point (647.096 K and 22.064 MPa) and surrounding regions.

IAPWS-95 is the most recent *general and scientific* model adopted by IAPWS. It is not to be confused with IAPWS-IF97 (Wagner et al., 2000), which is the corresponding *industrial formulation*. The industrial formulation is essentially a model fit to the IAPWS-95 model. It was created so that temperature and pressure are the primary variables, instead of temperature and density, the primary variables in IAPWS-95. The IAPS-84 and Keenan et al. (1969) models are analogous in this respect to IAPWS-95, having their own corresponding industrial formulations. The main purpose of the industrial formulations is to avoid the computational burden of iterative calculations required to solve temperature-pressure and similar types of problems using a model based on temperature and density.

Why use IAPWS-95 to compute thermochemical properties instead of using IAPWS-IF97? The former is more accurate (see Wagner and Pruss, 2002; Wagner et al., 2000). Maximum accuracy is desired as minor differences in thermochemical property values may significantly affect the results of thermochemical calculations. The use of the general and scientific model avoids a second issue with its corresponding industrial formulation. The latter uses different mathematical descriptions in different regions of temperature-pressure space, a characteristic that can result in inconsistencies at boundaries or small areas where regions may overlap (see Wagner et al., 2000). The present report does not compare of run times of software implementations of IAPWS-95 and IAPWS-IF97, but it is noted that the run times for problems run in developing and testing H2OI95 were trivial on a modern Windows PC.

H2OI95 is written in Fortran to assist with linking to SUPCRT92. As described here, it is a stand-alone code. The notion is that the main program can be replaced by an appropriate interface routine for incorporation into SUPCRT92 or similar software, using the remaining routines largely as-is, but eliminating much of the associated input/output needed for numerical studies. The FORTRAN used is relatively simple, such that translation into other computer languages should be relatively easy. All variable typing is explicit, and communication of variables among routines is made using only calling sequences.

Prior to developing H2OI95, a search was conducted for existing software for IAPWS-95 that might serve the purpose. Requirements were that the software be in Fortran or something close (such as C or C++), with available source code and no proprietary constraints or other problematic restrictions on usage. No such software was located. Consequently, H2OI95 was written following the model description given by IAPWS (2016). This description is more concise than that given by Wagner and Pruss (2002).

Three existing IAPWS-95 implementations were found that are nonetheless of special interest. One is a part of the NIST on-line Chemistry WebBook entitled "Thermophysical Properties of Fluid Systems" (http://webbook.nist.gov/chemistry/fluid/). If the selected species is "water," this web resource is an IAPWS-95 calculator. Because the user can specify the numerical precision desired in the results, this tool allows high-precision comparison with results from H2OI95 (more so than using the steam tables from Wagner and Pruss, 2002). However, the NIST WebBook does not calculate some properties of interest. The second implementation of interest here is the MATLAB application of Junglas (2008), which includes source code. This will be referenced regarding iterative approach, numerical analysis, and starting values for iterative calculations (but not for comparison of numerical results). The third implementation is a recent option in the computer code CHNOSZ (Dick, 2019). The default option for calculating water properties in this code is to use the models from SUPCRT92. CHNOSZ is written in the R language; it a incorporates much of the SUPCRT92 functionality. It has a particular focus on data/models for organic species and has diagraming capabilities not in SUPCRT92. It has a significant user base among geochemists. Dick (2019) describes the IAPWS-95 option as "meant for testing and model development purposes and is not recommended for routine use.". Comparing IAPWS-95 results from CHNOSZ with corresponding results from H2OI95 as illustrated in the present report would provide a rigorous testing of the CHNOSZ implementation, so that perhaps in the near future this might become the new default in CHNOSZ.

2. The IAPWS-95 Equation-of-State Model

The IAPWS-95 model (Wagner and Pruss, 2002) is based on the following model equation for the dimensionless Helmholtz energy:

$$A = \phi^o(\tau, \delta) + \phi^r(\tau, \delta)$$

This formulation divides the Helmholtz energy into an ideal part (ϕ^o) and a residual part (ϕ^r). Here τ is the *inverse* reduced temperature ($\tau = T_{cr}/T$) and δ is the reduced density ($\delta = \rho/\rho_{cr}$). Here T is the absolute temperature (K), ρ is density (kg/m^3), and the subscript "cr" refers to the critical point of water (647.096 K and 22.064 MPa pressure in this model). Also in this model, ρ_{cr} is 322 kg/m^3. The preceding general and scientific equation-of-state models noted previously also use some form of temperature and density as the primary variables, though they do not take this exact form. The Helmholtz energy is chosen to define the master equation because equations for all other thermodynamic functions can be obtained by applying various thermodynamic relations to the master equation. In general, these relations involve partial differentiation. A complete description of the relevant equations for the model is given by Wagner and Pruss (2002) and in condensed form by periodic "revised releases" put out by the International Association for the Properties of Water and Steam (IAPWS) on their web site. The most recent of these, IAPWS (2016), was followed in creating H2OI95. Note that IAPWS (2016, Table 1) gives slightly revised values for the constants n_1^o and n_2^o (compare with the original values given in Wagner and Pruss, 2002, Table 6.1).

The basic equations to first deal with in evaluating the model are the set of "ϕ" functions. These include ϕ^o and ϕ^r and their first and second order partial derivatives with respect to τ and δ. For the ideal function (ϕ^o) these partial derivatives are $\phi_\delta^o = \frac{\partial \phi^o}{\partial \delta}$, $\phi_{\delta\delta}^o = \frac{\partial^2 \phi^o}{\partial \delta^2}$, $\phi_\tau^o = \frac{\partial \phi^o}{\partial \tau}$, $\phi_{\tau\tau}^o = \frac{\partial^2 \phi^o}{\partial \tau^2}$, and $\phi_{\delta\tau}^o = \frac{\partial^2 \phi^o}{\partial \delta \partial \tau}$. Corresponding partial derivatives apply to the residual function (ϕ^r). See IAPWS (2016, Tables 4 and 5) for the equations to use in evaluating the ϕ functions. These are complex and require many constants (see IAPWS, 2016, Tables 1 and 2). The equations and constants are not given here.

IAPWS (2016, Table 3) gives equations for the basic thermodynamic functions (pressure, internal energy, entropy, etc.) in terms of the "ϕ" functions. For example, the pressure p (MPa) is given by

$$p = \rho R T (1 + \delta \phi_\delta^r)$$

where ρ (kg/m^3) and T (K) have been introduced previously, and R is the gas constant (0.46151805 kJ kg^{-1} K^{-1} for the IAPWS-95 model). The enthalpy h (kJ kg^{-1}) is given by

$$h = RT(1 + \tau(\phi_\tau^o + \phi_\tau^r) + \delta\phi_\delta^r)$$

and the entropy (kJ kg^{-1} K^{-1}) by

$$s = R\big(\tau(\phi_\tau^o + \phi_\tau^r) - (\phi^o + \phi^r)\big)$$

IAPWS (2016, Table 3) gives such formulas for thirteen thermodynamic properties, including the three noted above. It does not give the corresponding equation for the Gibbs energy g (kJ kg^{-1}). However, using the standard relation $g = h - T$s, one may obtain that

$$g = RT(1 + \phi^o + \phi^r + \delta\phi_\delta^r)$$

It also does not give the corresponding equation for the Helmholtz energy a (kJ kg^{-1}). However, this is given by the following minor modification of the previously noted master equation

$$a = RT(\phi^o + \phi^r)$$

The equations for p, a, and g are of special note here because their partial derivatives with respect to δ are useful in iterative calculations. These derivatives can be obtained from:

$$\frac{\partial p}{\partial \delta} = \frac{p}{\delta} + \rho_{cr} RT\delta(\phi_\delta^r + \delta\phi_{\delta\delta}^r)$$

$$\frac{\partial g}{\partial \delta} = RT(\phi_\delta^o + 2\phi_\delta^r + \delta\phi_{\delta\delta}^r)$$

$$\frac{\partial a}{\partial \delta} = RT(\phi_\delta^o + \phi_\delta^r)$$

Note that no “phi” functions are required other than those in the normally computed set.

3. Types of Problems: Inputs and Outputs

There are four basic types of problems in evaluating an equation-of-state models such as IAPWS-95. All are addressed by H2OI95. These problems are distinguished by the specified inputs:

1, Temperature (K) and density (ρ kg/m^3) or reduced density (δ)

2. Temperature (K) and pressure (MPa).

3. Temperature (K) on the saturation (liquid-vapor equilibrium) curve

4. Pressure (MPa) on the saturation curve

These types of problems are also addressed in SUPCRT92 (Johnson et al., 1992) and similar codes.

Problems are specified by text-based input files, examples of which will be noted later. H2OI95 expects an input file named "input". The code is run simply by entering its name, "`h2oi95`". Five pieces of output are produced. The first is screen output. This can be captured to a file using ">" when running the code. For example, "`h2oi95 > out`" captures the screen output on a file called "out". The screen output basically shows how the calculations are progressing. It does not include the full calculated results. Those are written to the "output" file, which is another text-based file. Included on this file are the "thermodynamic" or "thermophysical" results and the corresponding "thermochemical" results. The .csv files can be opened by any common spreadsheet or plotting program. The "thermodynamic" results are those which are native to the equation-of-state model, employing the units used in the model. These are the results that any equation-of-state solver would typically produce. Here for example entropy is on the model scale in which entropy is zero at the triple point and the calculated result is given in units of kJ kg^{-1} K. The "thermochemical" results are the results translated to standard thermochemical scales and corresponding units (see Appendix A for details). Here entropy is on the absolute or thermochemical scale and the result is given in units of kJ mol^{-1} K. The usual "thermodynamic" results are written to a comma-separated-variable (.csv) file called "mtab.csv", while the corresponding "thermochemical" results are written to another such file called "ctab.csv". Additional property results (see Section 5) are written to "xtab.csv".

3.1. Properties as a Function of Temperature and Density

The first type of problem is straightforward, as the inputs match the primary variables of the model. It is simply a matter of evaluating the model equations. In H2OI95, this is done by subroutine EVAI95. More commonly, the model user is interested in results for one of the other three problem

types. In these it is necessary to make iterative calculations, adjusting density values so that the problem inputs are satisfied. Direct calculation of properties from temperature and density can be very useful in numerical studies, as for determining ranges of convergence. It can also be useful in analyzing the potential problem of multiple numerical solutions for other types of problem inputs, as will be shown later in this report.

3.2 Calculating Properties as a Function of Temperature and Pressure

The IAPWS-95 model uses temperature and density as its primary variables. This choice facilitates correlation of data (development of an accurate model, as exemplified by IAPWS-95 and many other equation of state models for fluid substances). However, most model users are interested in thermodynamic and other properties as a function of temperature and pressure, not temperature and density. To calculate the properties for a given temperature and pressure, it is necessary to assume a starting value for density, calculate the corresponding pressure, and revise values of density and calculated pressure until the desired pressure is found. The most obvious method to apply to this problem is Newton-Raphson iteration (or some related method, such as the secant method). In the case of the Newton-Raphson method, one may write a residual function as

$$\alpha = p - p^*$$

where p is the pressure calculated from a value of δ and p^* is the desired pressure. The Newton-Raphson method generates a corrected value (δ_{i+1}, where i is iteration number) from the formula

$$\delta_{i+1} = \delta_i + c_i$$

where c_i is a correction term obtained from the equation

$$\left(\frac{\partial \alpha}{\partial \delta}\right) c_i = -\alpha_i$$

Here the partial derivative is evaluated using δ_i. This derivative constitutes the Jacobian matrix. Since this problem represents one equation in one unknown, the Jacobian is reduced to a scalar. It is apparent that

$$\frac{\partial \alpha}{\partial \delta} = \frac{\partial p}{\partial \delta}$$

where $\frac{\partial p}{\partial \delta}$ can be obtained as shown previously.

The convergence tolerance is generally placed on the relative error

$$\varepsilon_i = \frac{p_i - p^*}{p^*}$$

For thermochemical calculations, the tolerance itself should be rather tight, say $|\varepsilon_i| \leq$ x 10^{-9}. As will be noted, this is not always achievable, but when it is not, $|\varepsilon_i| \leq 1$ x 10^{-8} can generally be achieved.

In H2OI95 this type of calculation is solved by subroutine CALPRE. CALPRE makes successive calls to EVAI95 to evaluate the model equations. There are many ways that one might establish a starting value for δ. This value should be something that will facilitate rapid convergence to the desired solution, which is usually stable fluid satisfying certain constraints (discussed later). The default set of values provided in CALPRE generally appear to assure this. For any calculation for which the temperature is below the critical temperature, it is extremely helpful to know the densities of vapor and liquid on the saturation curve (as discussed later in conjunction with subroutine CALSCT). Thus one may appropriately determine values that are appropriate to vapor-like and liquid-like densities at the desired temperature. It is possible to run CALPRE with user-specified starting density values. This is typically done only in advanced work part of numerical studies. Results may then correspond to other than desired stable fluid (there is a multiple solutions problem), or the calculation may not converge.

The iterative process described above is essentially equivalent to that used in SUPCRT92 (Johnson et al., 1992), which uses for this purpose code borrowed from Haar et al. (1984) for use with the IAPS-84 model. Most if not all other examples of software for evaluating IAPS-84 or IAPWS-95 likely use the same or a similar approach. A somewhat different approach is used in the MATLAB application of Junglas (2008), who uses MATLAB's FZERO function to find an iterative solution. FZERO does not use Newton-Raphson, but rather the secant method and related methods that do not require evaluating a formula for a derivative.

The default starting density values provided in CALPRE are somewhat different from the starting values used in SUPCRT92 and Junglas' (2008) MATLAB application (2008). The general problem of starting values and the problems of multiple solutions and non-convergence will be addressed later in this report.

3.3 Calculating Properties on the Saturation Curve

The third and fourth types of problem deal with calculation of properties on the saturation (vapor-liquid equilibrium) curve, which extends from the triple point (273.16K, 0.611657 MPa) up to the critical point (647.096K, 22.064 MPa) (Figure 1). Usually the problem specifies a temperature value. It is then part of the problem to find the corresponding pressure and vapor and liquid densities. Less often, a pressure value is specified in place of one for temperature, in which case the problem includes finding the corresponding temperature.

The saturation curve represents a discontinuity of sort. If a third axis were to be added to represent density, the saturation curve would appear as sort of cliff, with higher values (liquid) above the curve and lower values (vapor) below it. The difference between the densities of liquid and vapor decreases going from the triple point to the critical point, decreasing rapidly near the critical point (Figure 2). What is shown in Figure 2 is not like a cliff or wall, but a gap. From the surface representing vapor, one could proceed through the gap onto the extended vapor surface underlying the liquid surface. Similarly, from the liquid surface, one could step out onto its extension overlying the vapor surface. Very close to the saturation curve, such extended surfaces represent metastable vapor and metastable liquid. The IAPWS-95 and similar models permit this, though most applications developed for the model do not support this. There are two points about this to keep in mind. First, how far these extensions go from the saturation curve is not well known. Second, no data for metastable fluids were used in developing the IAPWS-95 model, so accuracy would be expected to drop off rapidly moving away from the saturation curve.

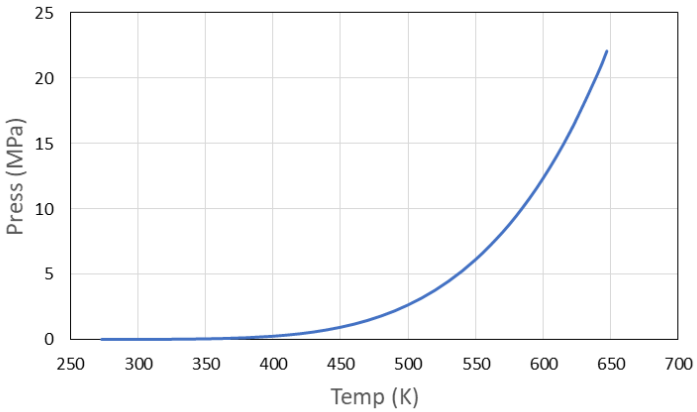

Figure 1. The saturation curve. The triple point is at the lower left end of the curve. The critical point is at the upper right end.

As shown in Figure 2, near the critical temperature (647.096K), the slope of density versus temperature becomes nearly infinite for the vapor curve and nearly negatively infinite for the liquid curve. The saturation curve on the density surface as would be represented by a three-dimensional plot of density versus temperature and pressure does not resemble a simple tear in the surface at the critical point; if it did, the slopes would approach a common finite value at the critical point. The actual behavior near the critical point is more like a tear combined with a very sharp fold; this is associated with extreme behavior of some thermodynamic functions (e.g., the heat capacity functions c_v and c_p) near the critical point.

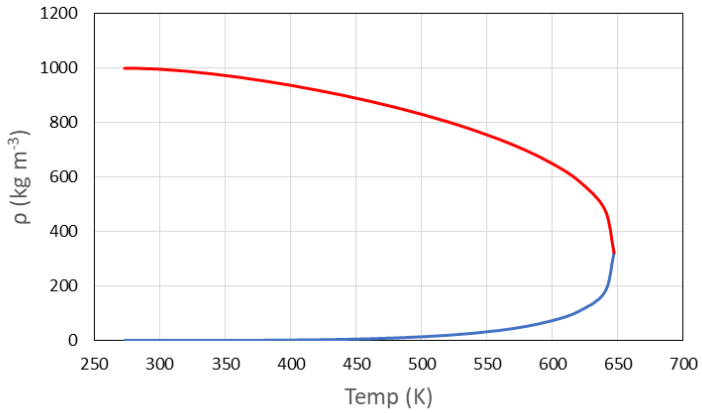

Figure 2. The density of vapor (blue) and liquid (red) on the saturation curve, as a function of temperature.

Wagner and Pruss (2002) cite equations describing the pressure and liquid and vapor densities on the saturation curve (their equations 2.5, 2.6 and 2.7). These equations are formally not part of IAPWS-95. However, they provide an excellent starting point for calculating values fully consistent with IAPWS-95. They are used for this purpose by Junglas (2008), and very likely by others as well. They will be referred to as the *saturation curve approximation*. An earlier saturation curve approximation also existed for IAPS-84 (Haar et al., 1984). It provided an estimate of the saturation pressure, but not estimates of the vapor and liquid saturation densities.

Consider the problem of finding the thermodynamic properties on the saturation curve where temperature is specified. It is desired to find the saturation pressure (p_S) and the vapor and liquid densities (δ_V and δ_L, respectively). The pressure equation previously introduced can be applied to each of vapor and liquid:

$$p_V = \rho_V RT\left(1 + \delta_V \phi_\delta^r(\tau, \delta_V)\right)$$

$$p_L = \rho_L RT\left(1 + \delta_L \phi_\delta^r(\tau, \delta_L)\right)$$

A third equation is required. The vapor and liquid are equilibrium on the saturation curve, therefore

$$g_V = g_L$$

Since these Gibbs energies can be calculated as functions of the respective densities using the Gibbs energy relation previously given, this provides a route to completing the saturation curve calculation. Noting that at saturation $p_V = p_L = p_S$, the right-hand sides of the above pressure equations can be combined to yield an equation in the densities, matching the dependency in a similar combination for the Gibbs energies. One then has two equations in two unknowns (the densities). Once this system of equations is solved, one can obtain the saturation pressure from either of the pressure equations.

This approach was used by Shi and Mao (2012), who initialize their calculations using the *saturation curve approximation* noted by Wagner and Pruss (2002). This approach appears to work well in this context. For computational details, see Shi and Mao's (2012) paper. The method is otherwise problematic, as other starting estimates can lead to undesired numerical solutions, such as convergence to the same fluid state for both "liquid" and "vapor." Such a final fluid state could technically be anywhere in the pressure-temperature field. The equation-of-state model itself only knows "fluid." It does not contain a built-in distinction between vapor and liquid. During the development of H2OI95, this numerical approach was tried and found sometimes to lead to such "single fluid state" results when the *saturation curve approximation* was not used to generate starting values.

To avoid this "single fluid state" issue, one generally uses some form of the so-called Maxwell criterion. This comes in different forms. James Clerk Maxwell's original analysis addresses a model cubic equation of state and deals directly with the notion of work (as in steam engines). A more direct approach for our purposes is to start with the Gibbs energy equality and replace Gibbs energy with Helmholtz energy. Recall that $g = a + pv$. Substituting this for vapor and liquid into the Gibbs energy equality and recognizing that there is only one pressure at saturation leads to:

$$p_M = \frac{(a_L - a_V)}{(v_V - v_L)}$$

where the calculated pressure here is marked as the "Maxwell" pressure. Because the difference of the specific volumes ($v = 1/\rho$) appears in the denominator, an iterative process accounting for this equation cannot converge to a numerical solution in which the "vapor" and "liquid" correspond to the same fluid

state. Although including a form of the Maxwell equation is better than omitting it, this still does not eliminate certain other kinds of undesired numerical solutions, for example one where metastable liquid (which is nearly incompressible) is in equilibrium with vapor for some pressure less than the saturation pressure. Thus, it remains important to initialize saturation curve calculations using the *saturation curve approximation*.

The final approach taken in H2OI95 is to define three residual functions in three unknowns (p_s, δ_V, and δ_S). The three functions are

$$\alpha_V = p_V - p_S$$
$$\alpha_L = p_L - p_S$$
$$\alpha_M = p_M - p_S$$

The equations are solved using Newton-Raphson iteration. A 3 x 3 matrix equation is solved for each iteration using Gaussian elimination (formulas for the Jacobian matrix are not given here but can readily be derived or inferred from the H2OI95 source code). Convergence testing is based on the largest magnitude relative error for the three residual functions. The normal convergence tolerance is 1 x 10^{-9}, the same value used in pressure-temperature calculations. The saturation curve problem for specified temperature is solved by subroutine CALSCT.

As found during testing, there are convergence issues between the triple point temperature (273.16K) and 298.15K and between 647.082K and the critical point temperature (647.096K). In the first instance, the convergence criterion is increased to 1 x 10^{-8}. In the second instance, the convergence criterion is increased to 1 x 10^{-7}. In addition, between 647.090K and the critical point temperature, iteration is otherwise stopped after five iterations. These accommodations were found necessary, as at some point further iteration would fail to result in any improvement. This is a characteristic of the equation of state itself in these regions, not something exhibiting a need for an improved numerical method. In the treatment of this kind of problem in SUPCRT92 (which uses the IAPS-84 model), there are similar accommodations. Special accommodations are also made by Junglas (2008) for his treatment of the IAPWS-95 model. In addressing the causes requiring these accommodations, Junglas points to the highly non-cubic form of the model. Further remarks on this subject will be made in Section 4.2, “Numerical Studies”.

The saturation curve problem for specified pressure is solved by subroutine CALSCP. The approach is to first estimate the corresponding temperature by inverting the *saturation curve approximation* equation for saturation pressure as a function of temperature. This is another iterative calculation (using the Newton-Raphson method). Once a temperature value is established, the next step is a CALSCT calculation to evaluate the calculated saturation pressure, which is then compared to the specified pressure. The temperature is then corrected using the secant method. This nested approach is less elegant than a direct approach, but it is easy to implement and likely nearly as fast as a direct approach. It avoids the need for certain ϕ functions (higher order derivatives) than are normally obtained. Also, this type of saturation curve problem is usually of less interest than the type in which the temperature is specified.

Others (Haar et al., 1984; Johnson et al., 1992: Junglas, 2008) use a different numerical approach in which the saturation pressure is first assumed known. The corresponding densities of vapor and liquid are then iteratively determined by applying the pressure equation separately to each phase. This is equivalent to two CALPRE calculations. The saturation pressure value is then adjusted using some form of the Maxwell criterion. Then the densities of the two phases are again determined. This continues until this nested iteration procedure converges. To adjust the saturation pressure value, Junglas (2008) uses the same Helmholtz energy-volume approach previously described. Haar et al. (1984) and Johnson et al. (1992) [who both address the IAPS-84 model, not IAPWS-95] use a different form based on Gibbs energy and the standard thermodynamic relation $\frac{\partial \Delta G}{\partial p} = -\Delta v$, where the "Δ" refers to the vapor-liquid transition.

4. IAPWS-95 Test Cases

A library ("Test_pkg") of test cases including examples of input files relevant to the present section and Section 5 is included with the software. In the present section, attention is focused on tests related to the IAPWS-95 EOS model. Section 5 discusses properties that can be calculated from this EOS model but are not addressed by Wagner and Pruss (2002) or IAPWS (2016). It also addresses properties that require supplementary or "add-on" models, such as for viscosity and dielectric constant. A general description of the test case library is given in Appendix B.

The present section focuses on common examples of the problem types most users of the IAPWS-95 EOS model would typically address. It further addresses more advanced examples of numerical studies, particularly of the issue of multiple numerical solutions for some EOS-related problems. Some numerical

results noted here required several runs over specific density ranges at varying density resolutions. Not all input files for these runs are included in the test case library accompanying the H2OI95 software.

4.1. Common Examples

This section addresses common examples of the type most code users would address. These also include cases addressing software verification. These examples include cases in which any starting values for density needed for iterative calculations are provided in the code itself. The results obtained correspond to what a user would ordinarily be seeking, that is, data for "stable" fluid such as one would find in steam tables.

4.1.1. The Properties of Liquid Water at 298.15K and 0.1 MPa

The following input file calculates the properties of (liquid) water at 298.15K and 1 bar (0.1 MPa) and at the same temperature and 1 atm (1.01325 bar or 0.101325 MPa). The number of temperature-pressure pairs that can be specified is not limited by the input file format.

```
Input_298
# VC298

# Calculate results for 298.15K and 1 bar pressure.
# The purpose is to validate the thermochemical results
# against the CODATA (Cox et al., 1989) recommendations
# for the thermochemical properties of water. For
# illustrative purposes, results are also obtained for
# 1 atm pressure (1.01325 bar). Pressure must be
# specified in MPa, not bars.

# The following strings are write option switches.

#showphi
#showdetails1
#showdetails2
#showdetails3

    tempk     press(MPa)
  298.150   1.000000000d-01
  298.150   1.013250000d-01
```

Lines beginning with "#" are treated as comment lines. The input file must begin with a line containing a name, usually the input file name (here `Input_298`). If the option strings shown in the example are not commented out, they will cause additional information to be written to the code output, which generally consists of screen output and the file named "output". The next essential line is the header line, here

containing the string "`tempk  press`". The "`(MPa)`" following "`press`" is optional and is there only as a reminder to input pressure in MPa units. Other potential units cannot be specified here. MPa units are intrinsic to the IAPWS-95 model and this software. Following the header are lines containing temperature-pressure pairs. Note that temperature must always be given in K.

Partial output (for 298.15K and 0.1 MPa only) is:

```
CALPRE: Temp(K) =  298.1500             tau    =  0.217037062E+01
        press   =  0.100000000E+00 MPa

   This appears to be liquid.

   CALPRE: iter=   0, px=  3.169929329E-03, sbetmx= -9.68301E-01
   CALPRE: iter=   1, px=  1.000099349E-01, sbetmx=  9.93490E-05
   CALPRE: iter=   2, px=  1.000000000E-01, sbetmx=  4.36567E-11

     Temp(K)           press(MPa)
    298.1500         0.100000000E+00

    H2O(liquid)

             delta           rho(kg/m3)
        0.309641938E+01   0.997047039E+03

      Thermodynamic Results

            u(kJ/kg)          h(kJ/kg)          s(kJ/kg/K)
        0.104818597E+03   0.104918893E+03   0.367199984E+00

            a(kJ/kg)          g(kJ/kg)          v(m3/kg)
       -0.466207858E+01  -0.456178241E+01   0.100296171E-02

          cv(kJ/kg/K)       cp(kJ/kg/K)          w(m/s)
        0.413756934E+01   0.418131883E+01   0.149669916E+04

           mu(K/MPa)       dt(kJ/kg/MPa)       bs(K/MPa)
       -0.221467031E-03   0.926024267E-06   0.184002805E-04

            av(/K)            kt(/MPa)
        0.257287426E-03   0.452463259E-03

      Thermochemical Results

           g(kJ/mol)         h(kJ/mol)         s(J/mol/K)
           -237.1403         -285.8300           69.9500

           a(kJ/mol)         u(kJ/mol)         v(m3/mol)
           -233.4724         -282.1621       1.80686E-05

         cv(J/mol/K)       cp(J/mol/K)     dt(kJ/mol/Mpa
           4137.5693         4181.3188        1.66826E-08
```

Here CALPRE is the subroutine that carries out this calculation. As shown, the calculation only required two iterations. The residual `betamx` is the relative error in the pressure. The normal convergence tolerance is 1 x 10^{-9}, which is very tight in part to support software verification. The high precision of the results shown is also intended to support verification. The thermochemical results for enthalpy (`h(kJ/mol)`) and entropy (`s(J/mol/K)`) exactly match the recommended CODATA (Cox et al., 1989) values. Here `rho` is density and `delta` (δ) is the reduced density (density divided by the critical point density). The other thermodynamic and thermochemical results shown use standard symbolic representation (e.g., `a` is Helmholtz energy, `g` is Gibbs energy, `cp` is heat capacity at constant pressure). Explanation of all symbols except `kt` (compressibility) is given by Wagner and Pruss (2002) and IAPWS (2016). Some of the thermodynamic and thermochemical values associated with the same symbol are different not only in units, but also tied to different arbitrary conventions. For example, this is true for the Gibbs energies, enthalpies, Helmholtz energies, internal energies (`u`), and entropies.

4.1.2. A Verification Test Case: Calculated "phi" Functions

Another type of input file is illustrated by the following verification test case. Most of the necessary discussion of what this test case is about is included in the input file itself. The basic purpose is to compare with high-precision values for the ϕ functions given by IAPWS (2016). Here the "`showphi`" option is active. Note that in this example, density ("`rho`") is specified instead of pressure. In this mode, density can also be specified as "`delta`". This type of calculation is done by subroutine CALDLT, which basically just calls EVAI95 to make a direct (non-iterative) evaluation of the equation-of-state model equations.

```
input_wt6
# VCwt6

# Compare results with Table 6 of IAPWS (2016), "Revised Release
# on the IAPWS Formulation 1995 for the Thermodynamic Properties
# of Ordinary Water Substance for General and Scientific Use".
# This document is available from the iapws.org web site as
# document IAPWS R6-95 (IAPWS95-2016.pdf). The purpose is to
# validate the calculation of the phi functions, for 500K and
# a density of 838.0250 kg/m3. Running the software with
# with "showphi" causes the phi functions to be written on the
# output. Density must be specified in kg/m3, not g/cm3.

# The contents of Table 6 from IAPWS (2016) partially duplicate
# Table 6.6 of Wagner and Pruss (2002). The latter table also
# includes a test at 647K and density of 358 kg/m3. Our results
# for phir, phird, and phirdd not precisely match theirs for
# these conditions. We believe it likely that IAPWS (2016)
```

```
# dropped this part of the original test for a reason, though
# they do not give one. This close to the critical point, minor
# differences may result from differences in numerical methods
# and tolerances. Results may also be compared with results
# (for liquid) from Table 13.1 of Wagner and Pruss (2002).
# However, their results are given to less precision.

# For the case at 500K and density of 838.0250 kg/m3, the result
# for phi0 given by Wagner and Pruss (2002) is off by one in the
# last decimal place from the value given by IAPWS (2016).

# The following strings are write option switches.

 showphi
#showdetails1
#showdetails2
#showdetails3

    tempk    rho(kg/m3)
  500.000   0.8380250d+03
  647.000   0.3580000d+03
```

The relevant output (for the 500K case is

```
       tempk =  0.500000000E+03   rho   =  0.838025000E+03
       delta =  0.260256211E+01   tau   =  0.129419200E+01



             phi functions

     phi0   =  0.204797733E+01     phir   = -0.342693206E+01
     phi0d  =  0.384236747E+00     phird  = -0.364366650E+00
     phi0dd = -0.147637878E+00     phirdd =  0.856063701E+00
     phi0t  =  0.904611106E+01     phirt  = -0.581403435E+01
     phi0tt = -0.193249185E+01     phirtt = -0.223440737E+01
     phi0dt =  0.000000000E+00     phirdt = -0.112176915E+01
```

UPDATE: The corresponding output for the 647K case obtained from version 1.1 is

```
       tempk =  0.647000000E+03   rho   =  0.358000000E+03
       delta =  0.111180124E+01   tau   =  0.100014838E+01



             phi functions

     phi0   = -0.156319605E+01     phir   = -0.121202657E+01
     phi0d  =  0.899441341E+00     phird  = -0.714012024E+00
     phi0dd = -0.808994726E+00     phirdd =  0.475730696E+00
     phi0t  =  0.980343918E+01     phirt  = -0.321722501E+01
     phi0tt = -0.343316334E+01     phirtt = -0.996029507E+01
     phi0dt =  0.000000000E+00     phirdt = -0.133214720E+01
```

These results exactly match those given in Table 6.6 of Wagner and Pruss (2002). Slightly different results had been obtained from version 1.0, as noted in the comments in the input file. Those comments do not apply to version 1.1.

4.1.3. Saturation Curve Properties as a Function of Temperature

The main "saturation curve" option (specified temperature or temperatures) is illustrated by the following input file:

```
input_sct
# VCsct

# Calculate results for specified temperatures along the
# saturation curve, using the "psat" option. The purpose
# is to compare results with those given in Table 13.1
# of Wagner and Pruss (2002).

# The following strings are write option switches.

#showphi
#showdetails1
#showdetails2
#showdetails3

    tempk    psat
  273.160
  274.000
  280.000
  300.000
  320.000
  340.000
  360.000
  380.000
  400.000
  420.000
  440.000
  460.000
  480.000
  500.000
  520.000
  540.000
  560.000
  580.000
  600.000
  620.000
  640.000
  647.096
```

This "`psat`" option utilizes specified temperature values (the last value is 647.096K, the critical point temperature). The saturation pressure and the properties of both saturated vapor and saturated liquid are

calculated. In H2OI95, the iterative calculation here is done by simultaneously solving three equations in three unknowns as described previously.

Convergence is illustrated by the following snippet of standard output:

```
  CALSCT: Temp(K) =  400.0000             tau    =  0.161774000E+01

     CALSCT: iter=   0, psat=  2.457652635E-01, betamx=  1.25696E-02
     CALSCT: iter=   1, psat=  2.457693473E-01, betamx=  6.81047E-08
     CALSCT: iter=   2, psat=  2.457693456E-01, betamx=  3.36722E-12

  CALSCT key results:

       Temp(K)          press(MPa)
      400.0000        0.245769346E+00

      H2O(vapor)

               delta           rho(kg/m3)
          0.425281845E-02   0.136940754E+01

      H2O(liquid)

               delta           rho(kg/m3)
          0.291144733E+01   0.937486039E+03
```

Here CALSCT is the subroutine that carries out this type of calculation. The final value of `press` is the calculated saturation pressure.

This is technically a verification test case, as one of the purposes is to calculate results that should match data included in Table 13.1 of Wagner and Pruss (2002). Agreement is essentially perfect, but comparison is not presented here because the Wagner and Pruss (2002) table gives results to only five or six significant figures, while a similar test case (VCwt8) based on Table 8 of IAPWS (2016) gives results with nine significant figures (see Section 4.3).

4.1.4. Saturation Curve Properties as a Function of Pressure

The other saturation curve option is that in which the pressure is specified instead of the temperature. An input file illustrating this is:

```
input_scp
# TCscp

# Calculate the saturation temperature and corresponding
# results for specified pressure values. This is an example
```

```
# of the "tsat" option. The purpose is to examine convergence
# behavior and to illustrate this option. Pressure must be
# specified in MPa, not bars.

# The following strings are write option switches.

#showphi
#showdetails1
#showdetails2
#showdetails3

   press(MPa)    tsat
   0.0100
   0.0500
   0.1000
   0.5000
   1.0000
   5.0000
  10.0000
  15.0000
  20.0000
```

This "`tsat`" option is implemented by making "`psat`" calculations for putative temperature values, and correcting the temperature to produce the specified pressure, using the nested approach described earlier. Correction of the temperature is done using the secant method, as previously noted. An advantage of this nested approach is that the calculation for any putative temperature utilizes coding in subroutine CALSTC that deals with the previously described issues regarding convergence in certain ranges of temperature.

A partial standard output snippet shows that convergence of the secant method is rapid:

```
  CALSCP: press  =  0.100000000E+00 MPa

     CALSCP: iter=   0, tempk= 372.7559, betamx=  4.27316E-07
     CALSCP: iter=   1, tempk= 374.7559, betamx=  7.36995E-02
     CALSCP: iter=   2, tempk= 372.7559, betamx=  1.24792E-08
     CALSCP: iter=   3, tempk= 372.7559, betamx=  6.66134E-15

  CALSCP key results:

       Temp(K)          press(MPa)
      372.7559        0.100000000E+00

      H2O(vapor)

               delta           rho(kg/m3)
          0.183336640E-02   0.590343980E+00

      H2O(liquid)

               delta           rho(kg/m3)
          0.297711648E+01   0.958631506E+03
```

Here CALSCP is the subroutine that carries out this type of calculation. Iteration in CALSTC done for each CALSCP iteration is not shown here.

Note that this is not a verification test case. It merely illustrates code capability.

4.2. Numerical Studies

The complexity of the equation-of-state model along with the need for iterative calculations to solve common problem types (e.g., specified temperature and pressure, specified temperature and saturation pressure, specified pressure and saturation temperature) suggests that there would be some minimum of pertinent literature regarding the numerical aspects of applying IAPWS-95 (or similar models, including the earlier IAPS-84 of Haar et al., 1984, and the even earlier model of Keenan et al., 1969). Such literature would focus on details of numerical methods, convergence properties including requirements on starting estimates of density, and an examination of the uniqueness and significance of numerical solutions. In fact, there is very little documented information of such studies. Haar et al., (1984) included code to evaluate the IAPS-84 model. Some details including starting estimates can be obtained from this. However, there is no discussion of how these values were established. Essentially the same coding is used in SUPCRT92 (Johnson et al., 1992). Junglas (2008) presented original numerical studies on the problem of obtaining saturation curve properties as a function of temperature but did not address the general case of specified pressure and temperature.

Wagner and Pruss (2002) presented no numerical studies, instead concentrating on how well the IAPWS-95 model reproduced experimental measurements. Clearly, they must have made some numerical studies in creating the software used to develop their model. Prof. Wagner made code available to academic investigators, but with restricted distribution and apparently no additional documentation. Obtaining results for stable fluid from iterative calculations is mainly dependent on the choice of starting values for density, and to a lesser degree on details of the iteration procedure. Precisely what Wagner and Pruss (2002) did in this regard seems to be undocumented, and no further information is given by IAPWS (2016).

Anyone developing an implementation of IAPWS-95 can do their own numerical studies, as did Junglas (2008) for saturation curve calculations. Additional numerical studies will be presented here, with a special focus on multiple numerical solutions and how to identify numerical solutions that are non-physical.

4.2.1. Multiple Solutions for Water at 500K and 25 MPa

The following input file was created for finding the properties of water at 500K (226.85^{o}C) and 25 MPa. The temperature is a "mid-range" value in relation to the saturation curve. The pressure is slightly higher than the critical pressure (22.064 MPa). Stable fluid in this region would commonly be referred to as "compressed liquid." This input file specifies the density values to use as starting estimates. The file was created by making multiple runs, trying various values. The process included finding "boundary" values for obtaining specific numerical solutions.

```
input_clx
# MCclx

# Calculate results for 500K and 25 MPa
# (in the compressed liquid field), specifying
# different starting values for the density
# (rhog, kg/m3). The purpose is to examine convergence
# behavior and to check for multiple solutions.
# Here three solutions are found, one of which
# is the expected solution for stable compressed liquid.
# The second solution might be thought of as corresponding
# to "compressed metastable vapor," although this represents
# an extrapolation and may not be accurate. It does not
# yield a valid result for the speed of sound. The third
# solution gives a negative absolute (thermochemical)
# entropy. Thus, it is a numerical solution with no
# realistic physical interpretation.
#
# The following strings are write option switches.

#showphi
#showdetails1
#showdetails2
#showdetails3

    tempk    press(MPa)        rhog(kg/m3)

# High density solution
  500.      25.00000000d+00    5000.
  500.      25.00000000d+00    2000.
  500.      25.00000000d+00    1100.
  500.      25.00000000d+00    1000.
  500.      25.00000000d+00    900.
  500.      25.00000000d+00    800.
  500.      25.00000000d+00    710.572

# Mid density solution
  500.      25.00000000d+00    710.571
  500.      25.00000000d+00    700.
  500.      25.00000000d+00    600.
  500.      25.00000000d+00    500.
```

```
  500.      25.00000000d+00    400.
  500.      25.00000000d+00    388.429

# No solution
  500.      25.00000000d+00    388.428
  500.      25.00000000d+00    385.
  500.      25.00000000d+00    380.
  500.      25.00000000d+00    375.703

# Low density solution
  500.      25.00000000d+00    375.702
  500.      25.00000000d+00    300.
  500.      25.00000000d+00    290.439

# No solution
  500.      25.00000000d+00    290.438
  500.      25.00000000d+00    200.
  500.      25.00000000d+00    100.
```

The pertinent results are that over a range of starting density values from 100 to 5000 kg/m^3, three solutions were found, each characterized by a specific range of starting values. Two ranges were also found in which no solution was found. Starting values from 710.572 to 5000 kg/m^3 led to a "high density" solution characterized by a final density of 850.558202 kg/m^3. Starting values from 388.429 to 710.571 kg/m^3 led to a "mid density" solution with a density of 621.049863 kg/m^3. Starting values from 290.439 to 375.702 kg/m^3 led to a "low density" solution with a density of 331.832991 kg/m^3.

When convergence was obtained, it was generally rapid, requiring 4-16 iterations. As would be expected, iteration number increased when starting farther from the obtained solution. Part of the screen output for the starting value of 2000 kg/m^3 illustrates convergence behavior:

```
  CALPRE: Temp(K) =  500.0000             tau    =  0.129419200E+01
          press   =  0.250000000E+02 MPa

          rhog    =  0.200000000E+04 kg/m3 (starting value)

     This appears to be compressed liquid.

     CALPRE: iter=   0, px=  2.238910656E+04, sbetmx=  8.94564E+02
     CALPRE: iter=   1, px=  6.488315591E+03, sbetmx=  2.58533E+02
     CALPRE: iter=   2, px=  2.008598643E+03, sbetmx=  7.93439E+01
     CALPRE: iter=   3, px=  6.061533203E+02, sbetmx=  2.32461E+01
     CALPRE: iter=   4, px=  1.729760662E+02, sbetmx=  5.91904E+00
     CALPRE: iter=   5, px=  5.224314248E+01, sbetmx=  1.08973E+00
     CALPRE: iter=   6, px=  2.690545502E+01, sbetmx=  7.62182E-02
     CALPRE: iter=   7, px=  2.501200918E+01, sbetmx=  4.80367E-04
     CALPRE: iter=   8, px=  2.500000049E+01, sbetmx=  1.95018E-08
     CALPRE: iter=   9, px=  2.500000000E+01, sbetmx= -2.10321E-14

       Temp(K)          press(MPa)
      500.0000        0.250000000E+02
```

```
 H2O(compressed liquid)

          delta           rho(kg/m3)
     0.264148510E+01   0.850558202E+03
```

The principal question is, what is the significance of three numerical solutions? The "mid density" solution was accompanied by the following messages from subroutine WROTAB:

```
WARNING (WROTAB): PRESSURE DERIVATIVE WITH RESPECT
   TO DENSITY IS LESS THAN ZERO. HAVE AN UNSTABLE SOLUTION.

WARNING (WROTAB): SPEED OF SOUND VALUE IS NOT POSITIVE.
   MAY HAVE A NON-PHYSICAL SOLUTION.
```

A negative value for the derivative of the pressure with respect to the density implies an unstable state (see for example Junglas, 2008). This condition is more often noted in conjunction with numerical solutions for density values that lie between the densities of vapor and liquid on the saturation curve, but it is not uniquely tied to that context. A negative value for this derivative corresponds to a negative value of the compressibility [$\kappa = \delta/(\partial p/\partial \delta)$]. In the IAPWS-95 model, the square of the speed of sound is calculated from the "phi" functions. In this instance, the square had a negative value. Therefore, a valid value for the speed of sound was not obtained. Therefore, the "mid density" solution is non-physical.

The "low density" solution was accompanied by the following message from subroutine WROTAB:

```
WARNING (WROTAB): THERMOCHEMICAL ENTROPY VALUE IS NOT POSITIVE.
   MAY HAVE A NON-PHYSICAL SOLUTION.
```

A thermochemical or absolute entropy must have a positive value. Therefore, the "low density" solution is also non-physical. A typical calculator for evaluating IAPWS-95 would not produce a value for the absolute entropy. In this situation, the non-physical nature of the "low density" solution might not be readily apparent if such a solution were to be calculated.

The "high density" solution shows no anomalies. Also, the results for this solution match the corresponding results given in the steam tables (Table 13.2) of Wagner and Pruss (2002). This is the desired solution. The results of this study indicate that a liquid-like density value is required to converge to the desired result. Per Table 13.1 of Wagner and Pruss (2002), the density of liquid on the saturation curve is 831.313 kg/m^3, which suggests a minimum value to use in the present case. Thus, when a calculation for the properties of water at any temperature below the critical temperature (647.096K) and any pressure is made, it is very useful in constructing appropriate starting density values to know the density values on the saturation curve. H2OI95 and probably most if not all other calculators for

IAPWS-95 and similar equation-of-state models calculate the saturation curve values for this purpose when solving this type of problem. Some may use values obtained from a saturation curve approximation; others, including H2OI95, use refined values starting from such. Either approach seems adequate.

Table 4.1 summarizes some of the key results from these calculations. In addition to the points already raised, the "low density" solution has a very low value for compressibility and a very high value for the speed of sound. The mid density solution has thermochemical entropy and Gibbs energy values similar to those of the "high density" solution. A key point to raise here is that the Gibbs energy value cannot be used to identify the desired solution. One might expect that the solution with the lowest such value would be the desired one, as this would seem to be the most thermodynamically stable. However, the "low density" solution here has the lowest Gibbs energy value, which is appears to be absurdly low.

Table 4.1. Partial results for water at 500K and 25 MPa. Cells highlighted in orange contain unrealistic results. Calculation of compressibility (κ) is addressed in Section 6.1. UPDATE: The compressibility values shown here are consistent with the specified units. See the Prologue for discussion of the pertinent error in Version 1.0 results.

Solution	ρ kg m^{-3}	κ MPa^{-1}	w m s^{-1}	S J kg^{-1} K^{-1}	G kJ mol^{-1}
High density	850.558202	$0.930558751 \times 10^{-3}$	$0.133010698 \times 10^{4}$	109.1009	-255.0398
Mid density	621.049863	$-0.487483957 \times 10^{-3}$	NC*	111.8598	-254.5668
Low density	331.832991	$0.275002785 \times 10^{-7}$	$0.338667401 \times 10^{6}$	-2.03222×10^{6}	-4.80574×10^{4}

*Not calculated ($w^2 \leq 0$)

An issue is how can one be confident that an IAPWS-95 software will consistently produce results for stable fluid from an iterative calculation, particularly when using a proprietary software whose details regarding exact iterative procedure and starting values for density are unknown. This concern is largely mitigated if the calculator has been extensively compared with the steam tables of Wagner and Pruss (2002, Tables 13.1 and 13.2). Presumably Wagner and Pruss took sufficient care to assure that the development of IAPWS-95 itself was not affected by convergence to any undesired numerical solutions. Although there seems to be no documentation directly addressing this point, the extensive comparison with experimental data in their paper strongly suggests that no problems of this type occurred.

4.2.2. Water at 500K over a Wide Range of Pressure

Another way of analyzing this problem is to calculate the curve of pressure versus density and note how many times the curve is intersected by the horizontal line representing the pressure of interest. Figure 3

shows the calculated curve for 500K over the density range 0 to 1200 kg/m^3 and for pressure in the range -400 to 1000 MPa. The full range of calculated pressure cannot be shown without losing necessary detail. The behavior of the curve is highly non-cubic. Calculated pressure can vary over many orders of magnitude and exhibits both positive and negative values. The pressure curve extends well beyond the boundaries of the figure. The three numerical solutions for 25 MPa (low, mid, and high density solutions) are marked on the diagram. The input file for this run is not given here, nor is it included in the test case package.

One can see that for higher pressures (up to at least 1000 MPa) and for somewhat lower pressure, there will also be three numerical solutions. For still lower pressures, the associated lines may intersect the portion of the pressure-density curve at lower density values (the part of the curve in the lower left-hand corner of Figure 3). Where that is the case, there may be up to five numerical solutions for a given pressure. It will be shown that, in general, only one solution is physically valid, or two, if the pressure is the saturation pressure for the given temperature.

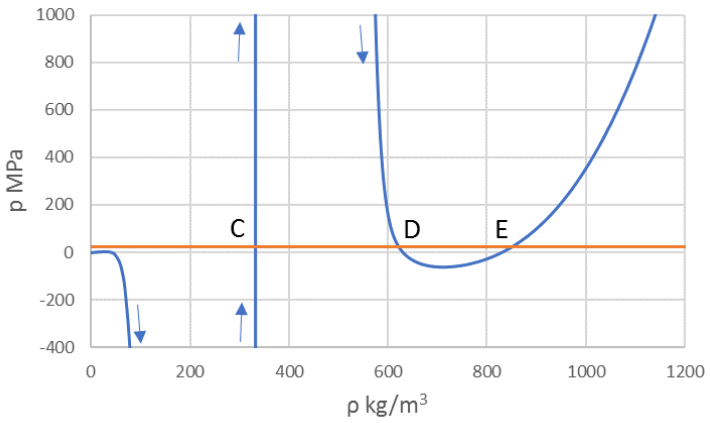

Figure 3. Pressure as a function of density (blue) at 500K. Arrows are shown to indicate curve direction moving outside the field of view. The line for 25 MPa is shown in red. For this pressure, C = low density solution, D = mid density solution, and E = high density solution.

Figure 4 depicts the part of the pressure curve in the bottom left portion of Figure 3. The violet line represents the saturation pressure (2.64 MPa). This is much lower than the 25 MPa shown by the red line in Figure 3. The 25 MPa line is not shown here because the pressure scale in Figure 4 only extends to 10 MPa. At saturation pressure, two numerical solutions are evident in this range. The higher density portion of the pressure curve in Figure 3 extends down past the saturation pressure (past zero pressure, for that

matter). Therefore, for the problem of finding solutions for the saturation pressure, there are another three numerical solutions (like C, D, and E in Figure 3, but adjusted to the saturation pressure).

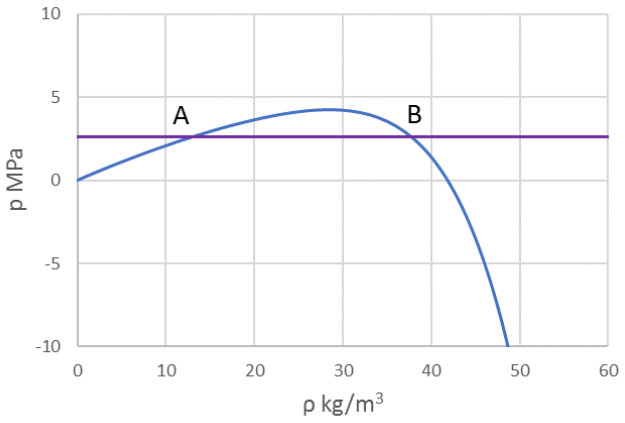

Figure 4. Pressure as a function of density (blue) and the saturation pressure (violet) at 500K. Points A and B mark numerical solutions in this range. Point A marks the physically valid solution for vapor. Point B marks an unstable solution (pressure decreasing with increasing density).

For slightly higher pressure for which the corresponding line would touch the top of the curve shown in Figure 4, there would be four numerical solutions. Above that pressure, there would be three such solutions (analogous to C, D, and E in Figure 3).

For the case of saturation pressure as exemplified in Figure 4 and implied by Figure 3, one would assume that the solutions for saturated vapor and saturated liquid are the only valid ones. To higher accuracy, the saturation pressure is 2.63919587 MPa. The five numerical solutions were calculated using this more accurate value. Point A represents the stable saturated vapor, while the adjusted (to the saturation pressure) point E represents the stable saturated liquid. Point B and the adjusted point D have negative slope of pressure versus density and are therefore unstable. In addition, point B has a negative value for the heat capacity at constant pressure, while the adjusted point D has a negative value for the square of the speed of sound. The adjusted point C has a negative value for the thermochemical (absolute) entropy. This non-physical solution has the lowest calculated Gibbs energy, again showing that the Gibbs energy cannot be used to identify a valid solution.

Some analysis is required to assure that any calculated numerical solutions have physical meaning. Four methods of disqualifying numerical solutions have been noted. These are (a) the calculated derivative of pressure with respect to density is negative, (b) a speed of sound value cannot be obtained because the

calculated square is negative, (c) the calculated thermochemical (absolute) entropy is not positive, and (d) the heat capacity at constant pressure (c_p) is not positive. A negative pressure itself is disqualifying, but one is not likely to specify a negative value for the desired pressure. Unfortunately, the lowest value of calculated Gibbs energy cannot be used to identify which of a set of numerical solutions corresponds to the desired one. There may be disqualifying factors in addition to those noted here, but these are the main ones that have been observed in testing H2OI95 and they appear to be sufficient.

The situation illustrated in Figure 3 is addressed by Wilhelmsen et al. (2017), who refer to it as the "Multiple Maxwell Loops" problem. A model with one "Maxwell loop" would behave much like a cubic equation of state (see the black curve in their Figure 3, which is for 550K, close to the 500K used here). The IAPWS-95 model curve in their Figure 3(b) [blue dashed line] closely resembles the curve shown in Figure 3 of the present report. Wilhelmsen et al. (2017) discuss out the existence of multiple numerical solutions. However, they mainly focus on approaches to modifying the mathematical structure of the equation of state to reducing the number of Maxwell loops (and numerical solutions), or at least minimizing the extreme behavior seen in Figure 3 of this report and their Figure 3 [again referring to the dashed blue line in their Figure 3(b)] iso that a resulting calculation of pressure as a function of density would look more like what would be obtained from a conventional cubic equation of state. Although the ideas they discuss are interesting, a practical alternative to IAPWS-95 avoiding non-physical solutions is still lacking.

4.2.3. Multiple Solutions for Water at 298.15K and 0.1 MPa.

The following input file was created for finding the properties of water at 298.15K (25^{o}C) and 0.1 MPa (1 bar), the thermochemical reference temperature and pressure. The temperature is a "low" value in relation to the saturation curve. The pressure is higher than the saturation pressure at this temperature. Stable fluid in this region would therefore be referred to as simply "liquid." This input file specifies the density values to use as starting estimates. The file was created by making multiple runs, trying various values. The process included finding "boundary" values for obtaining specific numerical solutions, using a method perhaps described as interval-halving by hand.

```
input_rtp
# MCrtp

# Calculate results for 298.15K and 1 bar pressure,
# specifying different starting values for the density
# (rhog, kg/m3). The purpose is to examine convergence
# behavior and to check for multiple solutions.
```

```
# Here two solutions are found, one of which is the
# expected solution for liquid water. The other
# solution can be interpreted as representing metastable
# vapor, although this is technically an extrapolation
# and may not be accurate.

# The following strings are write option switches.

#showphi
#showdetails1
#showdetails2
#showdetails3

    tempk    press(MPa)         rhog(kg/m3)
  298.150   1.000000000d-01    5000.
  298.150   1.000000000d-01    2000.
  298.150   1.000000000d-01    1000.
  298.150   1.000000000d-01    900.
  298.150   1.000000000d-01    894.327

  298.150   1.000000000d-01    894.326
  298.150   1.000000000d-01    800.
  298.150   1.000000000d-01    600.
  298.150   1.000000000d-01    400.
  298.150   1.000000000d-01    380.927

  298.150   1.000000000d-01    380.926
  298.150   1.000000000d-01    322.000
  298.150   1.000000000d-01    321.999
  298.150   1.000000000d-01    200.
  298.150   1.000000000d-01    100.
  298.150   1.000000000d-01    10.
```

The pertinent results are that over a range of starting density values from 10 to 5000 kg/m^3, two solutions were found, each characterized by a specific range of starting values. One range was also found in which no solution was found. Starting values from 894.327 to 5000 kg/m^3 led to a "high density" solution characterized by a final density of 997.047039 kg/m^3. Starting values from 380.927 to 784,325 kg/m^3 led to a "mid density" solution characterized by a density of 861.841021 kg/m^3. Starting values from 10 to 380.926 kg/m^3 did not lead to a numerical solution. In other words, no "low density" solution was found. However, it will be shown below that it does technically exist.

The mid density solution is not valid, as the derivative of pressure with respect to density is less than zero (indicating an unstable solution). Furthermore, this solution does not have a valid value for the speed of sound. The high density solution has no disqualifying characteristics and is thus the desired solution.

4.2.4. Water at 298.15K over a Wide Range of Pressure

Figure 3 shows the calculated pressure-density curve for 298.15 over the density range 0 to 1400 kg/m^3 and for pressure in the range -400 to 1000 MPa. As was the case for 500K, the full range of calculated pressure cannot be shown. The pressure curve again extends beyond the boundaries of the figure. The three numerical solutions for 25 MPa (low, mid, and high density solutions) are marked on the diagram. The corresponding input file is not given here o r included in the test case package.

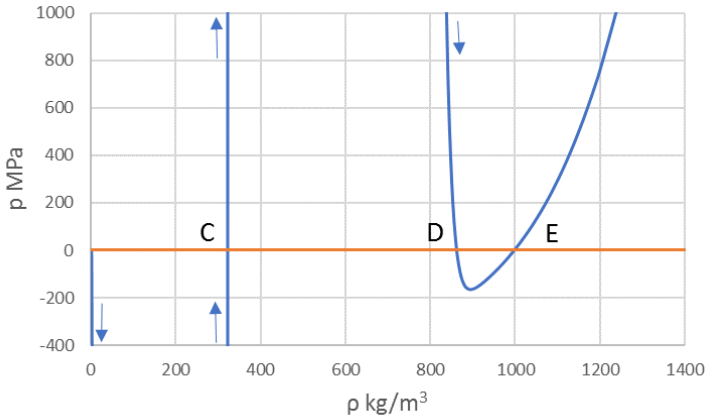

Figure 5. Pressure as a function of density (blue) at 298.15K. Arrows are shown to indicate curve direction moving across the field of view. The line for 0.1 MPa is shown in red. For this pressure, C = low density solution, D = mid density solution, and E = high density solution.

In section 4.2.3 (“MCrtp”), the iterative calculations to find numerical solutions failed to find the low density solution marked “C” in Figure 5. Additional iterative calculations were made to explore this issue. Starting with a density value of 321.999 kg/m^3 produced the following results taken from the output file:

```
CALPRE: Temp(K) =  298.1500             tau    =  0.217037062E+01
        press   =  0.100000000E+00 MPa

        rhog    =  0.321999000E+03 kg/m3 (starting value)

   This appears to be liquid.

   CALPRE: iter=   0, px= -1.295824659E+13, sbetmx= -1.29582E+14
   CALPRE: iter=   1, px=  1.408383723E+08, sbetmx=  1.40838E+09
   CALPRE: iter=   2, px= -8.780838300E+01, sbetmx= -8.79084E+02
   CALPRE: iter=   3, px= -8.780838300E+01, sbetmx= -8.79084E+02
   CALPRE: iter=   4, px= -8.780838300E+01, sbetmx= -8.79084E+02
   CALPRE: iter=   5, px= -8.780838300E+01, sbetmx= -8.79084E+02
   CALPRE: iter=   6, px= -8.780838300E+01, sbetmx= -8.79084E+02
   CALPRE: iter=   7, px= -8.780838300E+01, sbetmx= -8.79084E+02
   CALPRE: iter=   8, px= -8.780838300E+01, sbetmx= -8.79084E+02
```

```
   CALPRE: iter=   9, px= -8.780838300E+01, sbetmx= -8.79084E+02
   CALPRE: iter=  10, px= -8.780838300E+01, sbetmx= -8.79084E+02
   CALPRE: iter=  11, px= -8.780838300E+01, sbetmx= -8.79084E+02
   CALPRE: iter=  12, px= -8.780838300E+01, sbetmx= -8.79084E+02
   CALPRE: iter=  13, px= -8.780838300E+01, sbetmx= -8.79084E+02

 CALPRE: ITERATION IS NOT LEADING TO IMPROVEMENT.
   MAX NORM betamx =  8.791E+02, TOLERANCE btxtol =  1.000E-09
   MAX NORM dltamx =  2.107E-17, TOLERANCE deltol =  1.000E-12

 CALPRE: ITERATION FAILED.
```

The first pressure ("px") calculated corresponds to the starting density value. This pressure value is negative with quasi-infinite magnitude. Note that the calculated pressure appears to converge to a value of about -87.8084 MPa, which is not the desired pressure of 0.1 MPa.

A seemingly similar result is obtained for a starting density value of 322.000 kg/m^3. The corresponding results taken from the output file are

```
CALPRE: Temp(K) =  298.1500            tau    =  0.217037062E+01
        press   =  0.100000000E+00 MPa

        rhog    =  0.322000000E+03 kg/m3 (starting value)

   This appears to be liquid.

   CALPRE: iter=   0, px=  1.813818544E+09, sbetmx=  1.81382E+10
   CALPRE: iter=   1, px= -8.780838300E+01, sbetmx= -8.79084E+02
   CALPRE: iter=   2, px= -8.780838300E+01, sbetmx= -8.79084E+02
   CALPRE: iter=   3, px= -8.780838300E+01, sbetmx= -8.79084E+02
   CALPRE: iter=   4, px= -8.780838300E+01, sbetmx= -8.79084E+02
   CALPRE: iter=   5, px= -8.780838300E+01, sbetmx= -8.79084E+02
   CALPRE: iter=   6, px= -8.780838300E+01, sbetmx= -8.79084E+02
   CALPRE: iter=   7, px= -8.780838300E+01, sbetmx= -8.79084E+02
   CALPRE: iter=   8, px= -8.780838300E+01, sbetmx= -8.79084E+02
   CALPRE: iter=   9, px= -8.780838300E+01, sbetmx= -8.79084E+02
   CALPRE: iter=  10, px= -8.780838300E+01, sbetmx= -8.79084E+02
   CALPRE: iter=  11, px= -8.780838300E+01, sbetmx= -8.79084E+02
   CALPRE: iter=  12, px= -8.780838300E+01, sbetmx= -8.79084E+02
   CALPRE: iter=  13, px= -8.780838300E+01, sbetmx= -8.79084E+02

 CALPRE: ITERATION IS NOT LEADING TO IMPROVEMENT.
   MAX NORM betamx =  8.791E+02, TOLERANCE btxtol =  1.000E-09
   MAX NORM dltamx =  2.107E-17, TOLERANCE deltol =  1.000E-12

 CALPRE: ITERATION FAILED.
```

This resembles the results for the case shown previously. However, the first calculated pressure is now a positive number with very large, nearly quasi-infinite magnitude. The curve segment in Figure 5 associated with the problematic solution is a line with nearly infinite slope. Interestingly, the calculated

pressure similarly converges to the same incorrect value. Both calculations terminate with the report that "`MAX NORM dltamx =  2.107E-17`". The value reported here is the magnitude of the final Newton-Raphson correction, which about matches the machine epsilon for 64-bit arithmetic.

The problem here is that 64-bit arithmetic is insufficient to obtain convergence within normal tolerances for such a steep curve. Because all starting values close to the solution converge to the same finite pressure value, any attempt to further refine the precision of the starting estimates for density, as by interval halving, would be a futile exercise. The precision of the specified starting value would eventually run up against the machine epsilon (maximum allowed precision in the working calculations).

The part of the pressure-density curve in the lower left-hand corner of Figure 5 (which is barely visible there) is shown in expanded detail in Figure 6. This figure is analogous to Figure 4, which was for 500K. Two numerical solutions are found here at the saturation pressure of 3.16992934 x 10^{-3} MPa (the previous pressure of interest of 0.1 MPa is off the scale here). The solution on the left (A) is again the valid solution for saturated vapor, while the solution on the right (B) is an unstable solution. Point E from Figure 5, adjusted to the saturation pressure, is the valid solution for saturated liquid.

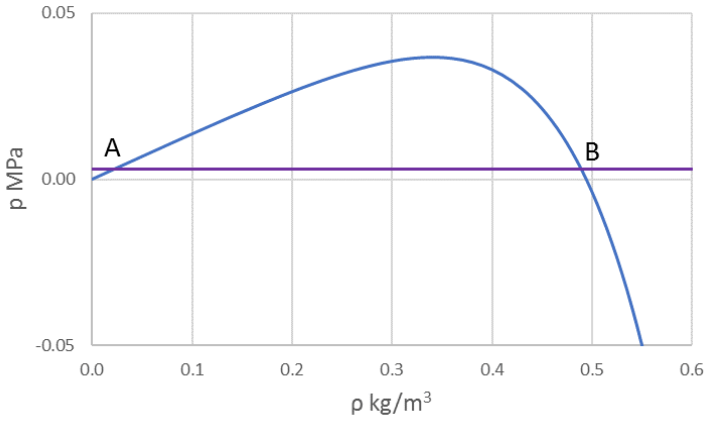

Figure 6. Pressure as a function of density (blue) and the saturation pressure (violet) at 298.15. Points A and B mark numerical solutions in this range. Point A corresponds to the physically valid solution for vapor, while Point B marks an unstable numerical solution.

4.2.5. Multiple Solutions for Water at 640K and 25 MPa

The following input file was created for finding the properties of water at 640K and 25 MPa. This temperature is several degrees below the critical temperature of 647.096K and slightly above the critical pressure of 22.064 MPa.

```
input_clf
# MCclf

# Calculate results for 640K and 25 MPa
# (in the compressed liquid field), specifying
# different starting values for the density
# (rhog, kg/m3). The purpose is to examine
# convergence behavior and check for multiple
# solutions. Here only one solution is found.
#
# The following strings are write option switches.

#showphi
#showdetails1
#showdetails2
#showdetails3

    tempk    press(MPa)        rhog(kg/m3)

# Unique density solution
  640.      25.00000000d+00    10000.
  640.      25.00000000d+00    5000.
  640.      25.00000000d+00    2000.
  640.      25.00000000d+00    1100.
  640.      25.00000000d+00    1000.
  640.      25.00000000d+00    900.
  640.      25.00000000d+00    800.
  640.      25.00000000d+00    700.
  640.      25.00000000d+00    600.
  640.      25.00000000d+00    500.
  640.      25.00000000d+00    442.515

# No solution
  640.      25.00000000d+00    442.514
  640.      25.00000000d+00    400.
  640.      25.00000000d+00    300.
  640.      25.00000000d+00    200.
  640.      25.00000000d+00    100.
  640.      25.00000000d+00    10.


# Version 1.0 split points
# 640.      25.00000000d+00    443.094
# 640.      25.00000000d+00    443.093
```

Only one numerical solution is found. Below it will be shown that there is indeed only one numerical solution (the valid one).

UPDATE: The input file for Version 1.1 was modified to change the boundary for the lowest starting density at which the single solution was found. As noted in the input file, this changed from 443.094 kg m^{-3} (the Version 1.0 result) to 442.515 kg m^{-3}.

4.2.6 Water at 640K over a Wide Range of Pressure

Figure 7 shows a plot of pressure versus density at 640K, using the same scale as in Figures 3 and 5. Also shown is the line (red) for a pressure of 25 MPa. The pressure-density curve here (blue) appears much better behaved, nearly monotonic at this scale. It appears to fall on the 25 MPa curve over much of the left-hand side of the figure. Figure 8 presents a close-up. Now it is clear that the nearly flat region of the pressure-density curve lies below the 25 MPa curve, closer in fact to the saturation pressure of 20.2652229 MPa, crossing the 25 MPa line at a single point (C). The corresponding input file input_640 is included in the test case package as part of test case PL640.

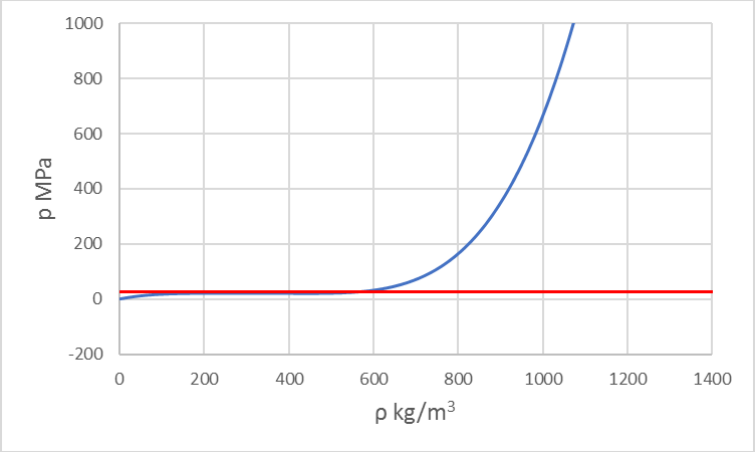

Figure 7. Pressure as a function of density (blue) at 640K. The line for 25 MPa is shown in red. No solution points are marked in this figure owing to the wide range of near overlap.

Figure 9 presents a much more detailed close-up (reduced pressure scale). The formerly flat-appearing curve segment shows significant curvature about the saturation pressure. Three numerical solutions are shown (points A, B, and C). Point A marks the solution for stable vapor and point C (the point C from Figure 8 but adjusted to the saturation pressure) marks the solution for stable liquid. The solution corresponding to point B is unstable. There is a near solution marked X. At a slightly lower pressure, say 20.2 MPa, two additional numerical solutions would appear. It can be shown that these would be non-physical using the methods previously discussed.

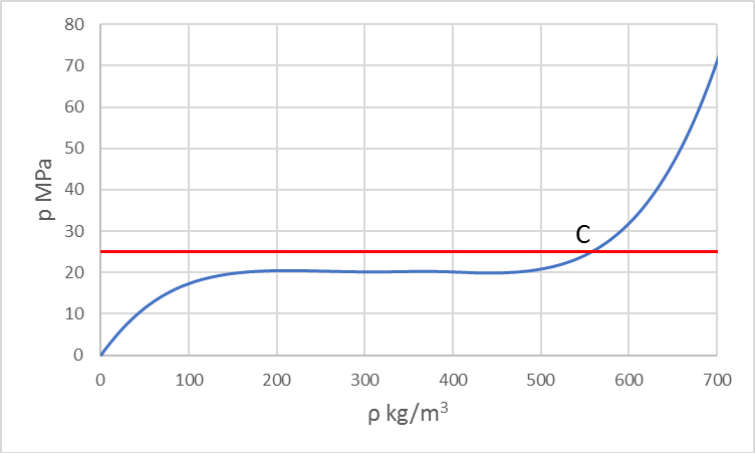

Figure 8. Pressure as a function of density (blue) at 640K, expanding the area where the area where the calculated pressure is close to 25 MPa (red line). There is a single solution point ("C").

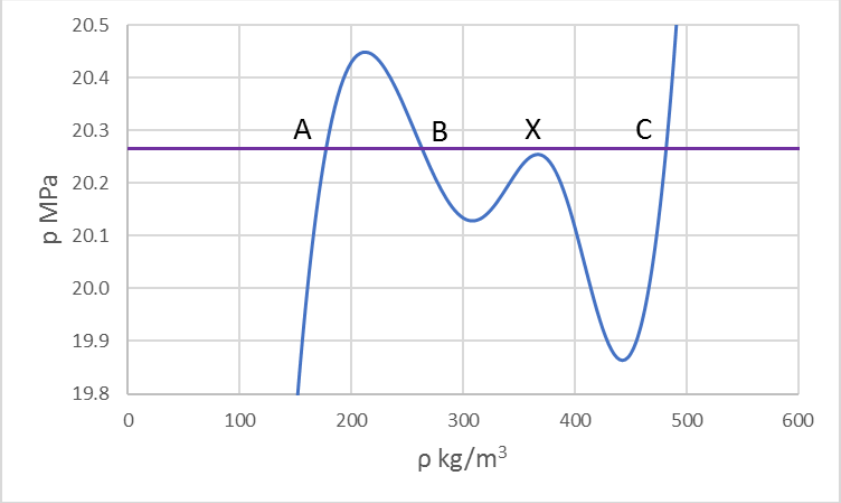

Figure 9. Pressure as a function of density (blue) at 640K, expanding the area where the curve appears nearly flat in Figure 8. On the present scale, it appears very much not flat. The violet line marks the saturation pressure. Three numerical solutions are apparent. The blue line does not touch or cross the violet line near the point marked "X".

UPDATE: Although the temperature here is close to the critical temperature (647.096K) and the conditions shown Figures 7, 8, and 9 pass near the critical point, the curves shown here are virtually indistinguishable from those generated using Version 1.0.

4.2.7. Water at 655K over a Wide Range of Pressure

Figure 10 shows a plot of pressure versus density at 655K (above the critical point), using the same scale as in Figures 3, 5, and 7. No special pressure line is shown. The pressure-density curve here (blue) appears monotonic at this scale. That was also the case for 640K, although in that case analysis showed non-monotonicity at finer scale. The curve differs significantly from that expected for ideal gas (red line, $P = \rho RT$). Figure 11 presents a close-up of the blue curve analogous to Figure 9. In this case (655K), there is clear monotonicity, implying only one numerical solution for any given pressure. The input file used to generate these figures is not given here, nor is it in the test case library.

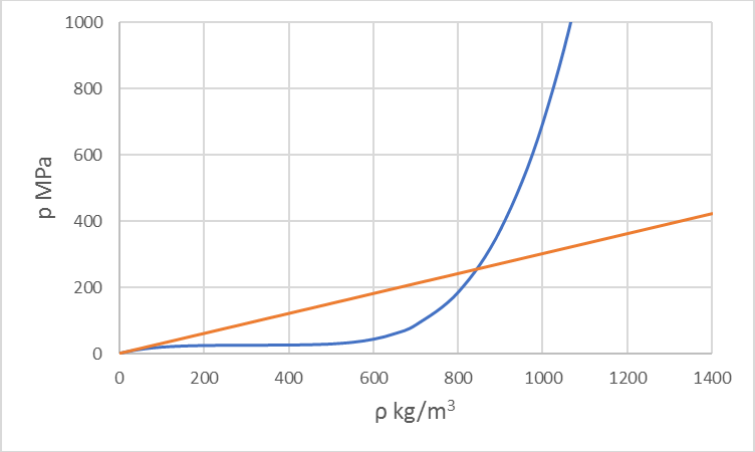

Figure 10. Pressure as a function of density (blue) at 655K. The ideal gas pressure is shown by the red line.

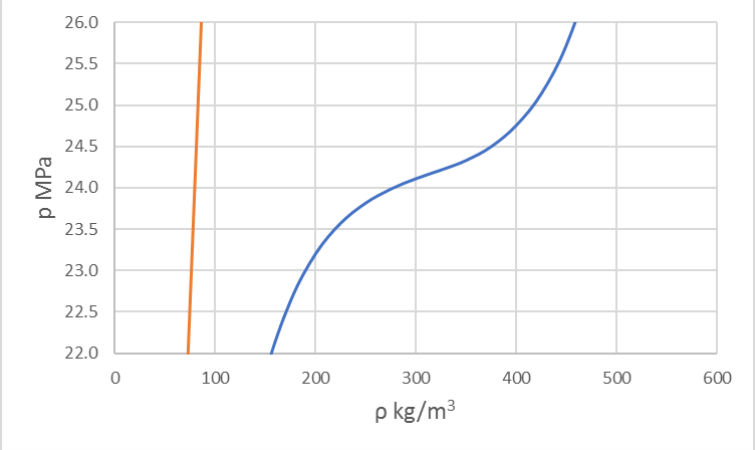

Figure 11. Pressure as a function of density (blue) at 655K, expanding the area where the curve appears nearly flat in Figure 10. The curve is clearly monotonic on this finer scale. The ideal gas pressure is shown by the red line.

It can be shown that at still higher temperature, the pressure curve remains monotonic.

4.2.8. Water at 800K over a Wide Range of Pressure

Figure 12 shows a plot of pressure versus density at 800K (well above the critical point), using the same scale as in Figures 3, 5, 7, and 10. The pressure-density curve here (blue) appears monotonic. The curve still differs significantly from the pressure expected from an ideal gas (red line). Figure 13 presents a close-up view analogous to Figures 9 and 11. This confirms monotonicity of the blue curve. The calculated behavior more clearly converges with that of ideal gas (red line) at sufficiently low pressure. The input file used to generate these figures is not given here, nor is it in the test case library.

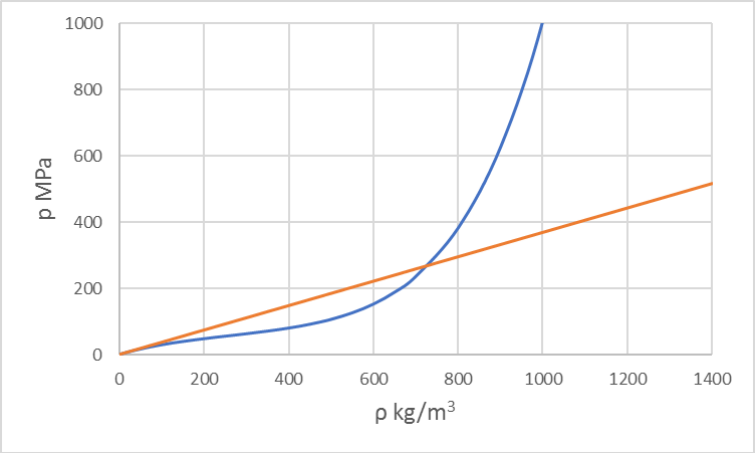

Figure 12. Pressure as a function of density (blue) at 800K. The red line shows the behavior of ideal gas.

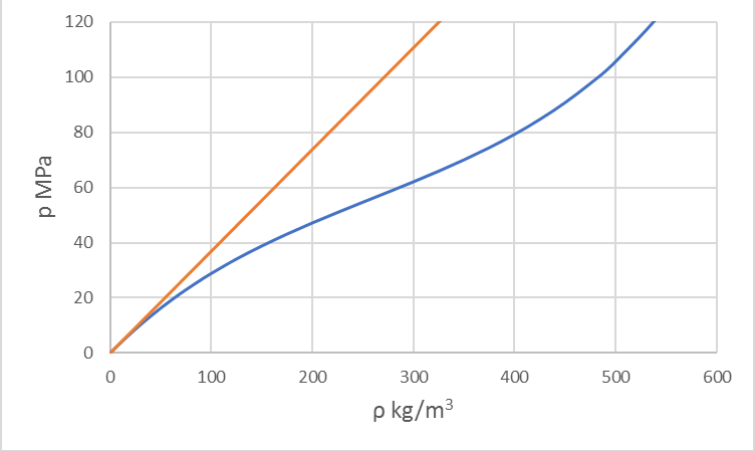

Figure 13. Pressure as a function of density (blue) at 800K, expanding the area in the lower left corner of Figure 12 (low density and low pressure). The red line again shows the behavior of ideal gas. Monotonicity of the blue curve is quite clearly apparent. Also apparent is the approach of the blue curve to ideality at very low density and pressure.

Although monotonicity is a characteristic of pressure as a function of density at temperatures above the critical temperature, ideal gas behavior is approached only at rather low pressure.

Due to the mathematical complexity of the IAPWS-95 model and the fact that the model is only calibrated in a specific range of temperature and pressure, any extrapolation outside that range (especially to higher pressure) should be done with care. Additional numerical studies would be recommended.

4.3. Verification of the Implementation of IAPWS-95 in H2OI95

The primary verification of the IAPWS-95 implementation in H2OI95 is associated with three test cases: VCwt6, VCwt7, and VCwt8. These are respectively associated with Tables 6, 7, and 8 of IAPWS (2016). VCwt6, described in Section 4.1.2, is also associated with Table 6.6 of Wagner and Pruss (2002). These test cases are those recommended by IAPWS (2016). They are further significant in that results are presented to nine significant figures, better than the five to six significant figures found in the steam tables (Tables 13.1 and 13.2) of Wagner and Pruss (2002).

As previously noted in Section 4.1.2, the purpose of VCwt6 is to check calculated values of "phi" functions. Comparison with H2OI95 version 1.1 results showed a match to the nine significant figures for the two cases given in Table 6.6 of Wagner and Pruss, while version 1.0 results matched for the first case (the only one in Table 6 of IAPWS, 2016), but did not match as well for the second case.

The purpose of VCwt7 is to compare results for a limited set of properties for a small number of temperature and density values given in Table 7 of IAPWS (2016). This can thought of as a reduced form of Table 13.2 of Wagner and Pruss (2002). The density values (inputs) are given by IAPWS (2016) to eight significant figures, while the other property values are given to nine. Corresponding results from H2OI95 are shown in the following snippet, arranged to match the layout of the table from IAPWS (2016).

Temp(K)	rho(kg/m3)	Press(MPa)	cv(kJ/kg/K)	w(m/s)	s(kJ/kg/K)
300	9.9655600E+02	9.92418352E-02	4.13018112E+00	1.50151914E+03	3.93062643E-01
300	1.0053080E+03	2.00022515E+01	4.06798347E+00	1.53492501E+03	3.87405401E-01
300	1.1882020E+03	7.00004704E+02	3.46135580E+00	2.44357992E+03	1.32609616E-01
500	4.3500000E-01	9.99679423E-02	1.50817541E+00	5.48314253E+02	7.94488271E+00
500	4.5320000E+00	9.99938125E-01	1.66991025E+00	5.35739001E+02	6.82502725E+00

500	8.3802500E+02	1.00003858E+01	3.22106219E+00	1.27128441E+03	2.56690919E+00
500	1.0845640E+03	7.00000406E+02	3.07437693E+00	2.41200877E+03	2.03237509E+00
647	3.5800000E+02	2.20384756E+01	6.18315728E+00	2.52145078E+02	4.32092307E+00
900	2.4100000E-01	1.00062559E-01	1.75890657E+00	7.24027147E+02	9.16653194E+00
900	5.2615000E+01	2.00000690E+01	1.93510526E+00	6.98445674E+02	6.59070225E+00
900	8.7076900E+02	7.00000006E+02	2.66422350E+00	2.01933608E+03	4.17223802E+00

The comparison shows an exact match to the nine significant figures, except for the pressure calculated for 500K and density of 1.0845640E+03 kg m^{-3} (the highlighted value). There is a difference of unity in the last digit, which appears to be due to a difference in rounding practice.

The purpose of VCwt8 is to compare results for some properties at a limited number of temperatures and saturation curve pressure as given in Table 8 of IAPWS (2016). This can thought of as a reduced form of Table 13.1 of Wagner and Pruss (2002). The requisite property values are given to nine significant figures. Corresponding results from H2OI95 are shown in the following snippet, arranged to match the layout of the table from IAPWS (2016).

Temp(K)	275	450	625
Press(MPa)	6.98451167E-04	9.32203564E-01	1.69082693E+01
rho(kg/m3) liq	9.99887406E+02	8.90341250E+02	5.67090385E+02
rho(kg/m3) vap	5.50664919E-03	4.81200360E+00	1.18290281E+02
h(kJ/kg) liq	7.75972202E+00	7.49161585E+02	1.68626976E+03
h(kJ/kg) vap	2.50428995E+03	2.77441078E+03	2.55071625E+03
s(kJ/kg/K) liq	2.83094670E-02	2.10865845E+00	3.80194683E+00
s(kJ/kg/K) vap	9.10660121E+00	6.60921221E+00	5.18506121E+00

The comparison shows an exact match to the nine significant figures.

The above verification test cases are the only ones recommended by IAPWS (2016), and VCwt6 is the only one explicitly recommended by Wagner and Pruss (2002).

As noted, Wagner and Pruss (2002) give extensive steam tables in their Table 13.1 (saturation curve) and Table 13.2 (single phase, specified temperatures and pressures). However, they only give values to five or six significant figures. Test case VCsct was created to allow partial comparison with values from Wagner and Pruss (2002, Table 13.1) and test case VCpre was similarly created to allow partial comparison with values from Wagner and Pruss (2002, Table 13.2). The resulting comparisons, to the number of significant figures given by Wagner and Pruss (2002), are exact for H2OI95 version 1.1, allowing for a

possible unit different in the last digit, to account for rounding differences. Those comparisons are not presented here. They are considered verification at a second level. It is noted that for H2OI95 version 1.0, results for VCsct at 640K (close to the critical point) were very slightly off.

Other verification test cases pertinent to the IAPWS-95 implementation are included in the distributed library, not all of which are discussed in the present report. Some involve comparison with results from other sources, including results based on models other than IAPWS-95 (for which only approximate matches are deemed sufficient). Some verification activity has involved comparison with high-precision results obtained from the NIST on-line calculator "Thermophysical Properties of Fluid Systems" (http://webbook.nist.gov/chemistry/fluid/).

It was thought in the development of H2OI95 version 1.0 that the primary verification test cases described above were sufficient to assure accurate implementation of the IAPWS-95 model. In implementing the viscosity model described in Section 5.2.1, it was found that this was not the case. A verification test of the calculated dimensionless isothermal compressibility (needed to calculate the viscosity) is also required. This compressibility is described in Section 5.1.3. Table 5.4 presents results that should be used in the related verification test.

The problem in version 1.0 of H2OI95, as discussed in Section 5.2.1 and Appendix C, is a coding error affecting mainly "higher-order" properties such as compressibility and isobaric heat capacity close to the critical point. Although a specific verification test is noted in Section 5.1.3, it was wondered whether or not the problem could have been detected using the steam tables (Tables 13.1 and 13.2) of Wagner and Pruss (2005). The test cases VCwt7, VCwt8, VCstc, and VCpre discussed previously covered ground related to these tables. However, they did not cover sufficient ground close to the critical point. Only the 640K point in VCstc showed any sign of a potential problem, and the differences seen were small enough that they might have been due to differences in computing environment (exact coding, compilers, compile options, or characteristics of numerical processors). It is noted that Wagner and Pruss (2002) noted such possible cause of differences. Also, they did not suggest specific criteria for verification purposes. The critical point itself does appear in these test cases. However, the problem noted here does not manifest at the critical point itself.

To obtain a more detailed look close to the critical point, two additional test cases were created. Results were obtained from both versions 1.0 and 1.1 of H2OI95, with the goal of assessing how useful the steam tables might have been in detecting the error in version 1.0. VCwp1 addresses at points on the saturation

curve (Wagner and Pruss, 2002, Table 13.1), specifically at 636, 638, 640, 642, 644, 646, 647, and 647.096K (the critical temperature). VCwp2 addresses points for 22.5 MPa from Wagner and Pruss (2002, Table 13.2). This pressure is the closest in that table to the critical pressure (22.064 MPa). The temperatures are 620, 630, 640, 650, and 675K. The results obtained from version 1.1 were found to be identical to the steam table values in Wagner and Pruss (2002) to the precision given in the latter.

Results for VCwp1 are shown for density (Table 4.2) and isobaric heat capacity (Table 4.3). The data shown here is for the liquid on the saturation curve (relative differences for the vapor are smaller). What is significant here is that there is are definite trends in the differences of version 1.0 values on the one hand and version 1.1 (or Wagner and Pruss, 2002. Table 13.1) values on the other. This makes a strong case that the version 1.0 implementation of IAPWS-95 contains an error.

Table 4.2. Density results for liquid obtained from VCwp1 from H2OI95, versions 1.1 and 1.0.

	ρ(kg m^{-3})			
Temp(K)	v. 1.1	v. 1.0	Diff.	%. Diff.
636	510.42	510.43	0.01	0.002
638	496.82	496.85	0.03	0.006
640	481.53	481.60	0.07	0.015
642	463.67	463.81	0.14	0.030
644	440.73	440.86	0.12	0.028
646	402.96	401.54	-1.42	-0.352
647	357.34	355.07	-2.27	-0.635
647.096	322.00	322.00		

Table 4.3. Isobaric heat capacity results for liquid obtained from VCwp1 from H2OI95, versions 1.1 and 1.0.

	c_p(kJ kg^{-1} K^{-1})			
Temp(K)	v. 1.1	v. 1.0	Diff.	%. Diff.
636	17.995	18.007	0.012	0.065
638	21.122	21.163	0.042	0.197
640	25.942	26.091	0.148	0.572
642	34.929	35.479	0.550	1.574
644	58.910	61.406	2.495	4.236
646	204.58	214.53	9.945	4.861
647	3905.2	3294.7	-610.5	-15.632
647.096	qINF*	qINF*		

*quasi-infinite

For density and isobaric heat capacity (and other calculated properties not shown here), the differences are relatively small until a few degrees from the critical point. The largest relative errors are for the isobaric heat capacity, which like compressibility, is a "higher-order" property (calculated using the higher-order derivatives of the ϕ function).

Results for VCwp2 are shown for density (Table 4.4) and isobaric heat capacity (Table 4.5). Below the critical temperature (647.096K), the relevant fluid is compressed liquid; above it, the fluid is supercritical. In the case of the density, there are no differences at 620, 630, and 675K. There is a notable difference for 650K, and a small one for 640K. This is more or less typical of the other properties calculated. Where differences exist, they are again largest for the isobaric heat capacity (table 4.3Unfortunately, Table 13.2 of Wagner and Pruss (2002) does not give finer resolution of temperature.

Table 4.4. Density results obtained from VCwp2 from H2OI95, versions 1.1 and 1.0.

	ρ(kg m^{-3})			
Temp(K)	v. 1.1	v. 1.0	Diff.	% Diff.
620	625.149	625.149	0.000	0.000
630	586.927	586.927	0.000	0.000
640	531.385	531.387	0.002	0.000
650	218.278	218.212	-0.066	-0.030
675	124.868	124.868	0.000	0.000

Table 4.5. Isobaric heat capacity results obtained from VCwp2 from H2OI95, versions 1.1 and 1.0.

	c_p(kJ kg^{-1} K^{-1})			
Temp(K)	v. 1.1	v. 1.0	Diff.	% Diff.
620	7.1128	7.1128	0.0000	0.0000
630	8.4284	8.4284	0.0000	0.0000
640	12.1420	12.1431	0.0010	0.0086
650	65.2717	65.5580	0.2863	0.4387
675	8.1990	8.1990	0.0000	0.0000

Results obtained from version 1.1 of H2OI95 indicate that for verification testing of software using 64-bit arithmetic the following criterion should be applied. Value pairs should agree to the last significant figure of the baseline (assumed correct) value, with an acceptable difference of plus or minus one in the last significant digit to account for possible differences in rounding/truncation. The number of such significant digits can be at least nine, as in test cases VCwt6, VCwt7, and VCwt8. In theory, one might do better with 64-bit arithmetic. However, nine digits is consistent with the usual convergence criterion of 1×10^{-9}.

It is suggested that all of the verification test cases used in this report (those in the "VC" category) be used in computer verification of any other software using the same models (IAPWS-95 and supplementary models). Verification associated with properties described in Section 5 is presented in that Section.

5. Additional Properties

The IAPWS-95 model (Wagner and Pruss, 2002) as described by IAPWS (2016) with minor modification has been implemented in the program H2OI95. The original version of H2OI95 (v. 1.0) calculates those properties for which formulas are given by the above sources. However, the equation-of-state model can provide additional thermodynamic properties using the appropriate definitions and thermodynamic relations. These properties include the isothermal compressibility (κ_T) and the isobaric thermal expansivity (α_p). Other properties, including the dynamic viscosity, thermal conductivity, surface tension, and dielectric constant, can be found using additional models sanctioned by the IAPWS. From these properties, still more properties can be obtained. For example, Debye-Hückel constants and Born functions (discussed by Helgeson and Kirkham, 1974b) can be obtained from the dielectric constant and other properties. H2OI95 v. 1.1 calculates a number of additional properties, outputting them on the new xtab.csv file.

5.1. Additional Properties Obtained Directly from the IAPWS-95 Model

The properties of interest here include the isothermal compressibility and the isobaric thermal expansivity. Complete formulas for calculating these properties from the equation-of-state model were not given by Wagner and Pruss (2002) or IAPWS (2016), probably because no measurements of such were used to construct the model. To obtain experimental values for these properties, one would be measuring specific volume or density as a function of temperature and pressure, and then numerically differentiating the volume function. The IAPWS-95 model is based instead on what would be the original volume or density data. Data for isothermal compressibility and isobaric thermal expansivity might be used in geochemical or engineering applications to extrapolate Gibbs energies and other thermodynamic functions from reference temperature and pressure, commonly 25°C and 0.1 MPa (1 bar) to higher temperatures and pressures. However, with an equation-of-state model, they are not needed for this purpose, as the EOS model can directly provide values of Gibbs energies and other thermodynamic functions at any desired temperature and pressure in the range of the model. Nevertheless, there may be

interest in these properties for other reasons, such as providing or establishing correlations with other kinds of properties. Also, they might be needed as inputs to calculate other properties from certain models. For example, the dimensionless isothermal compressibility function ζ_T, which is related to the isothermal compressibility κ_T, is a required input to the IAPWS (2008) viscosity model and the IAPWS (2011) thermal conductivity model.

5.1.1. Isothermal Compressibility

The isothermal compressibility is defined by:

$$\kappa_T = -\frac{1}{v}\left(\frac{\partial v}{\partial p}\right)_T$$

It has dimensions of inverse pressure. An equivalent formula in terms of density is:

$$\kappa_T = \frac{1}{\rho}\left(\frac{\partial \rho}{\partial p}\right)_T$$

Substituting $1/v$ for ρ in the second equation and evaluating the resulting derivative leads to the first equation given above. Noting that $\delta = \rho/\rho_{cr}$ means that $\rho = \rho_{cr}\delta$, hence one can substitute $\rho_{cr}\delta$ for ρ in the second equation given above and obtain

$$\kappa_T = \frac{1}{\delta}\left(\frac{\partial \delta}{\partial p}\right)_T$$

One can then use the partial derivative relation

$$\left(\frac{\partial \delta}{\partial p}\right)_T = \left(\frac{\partial p}{\partial \delta}\right)_T$$

to obtain

$$\kappa_T = {1}\Big/{\delta\left(\frac{\partial p}{\partial \delta}\right)_T}$$

The partial derivative here is the same one used in Newton-Raphson iteration to find the value of δ corresponding to a desired pressure. The formula for this was previously given as

$$\frac{\partial p}{\partial \delta} = \frac{p}{\delta} + \rho_{cr} RT\delta(\phi_\delta^r + \delta\phi_{\delta\delta}^r)$$

No direct means were found to validate calculated results, in the sense that no tables were found that tabulate compressibility values calculated from the IAPWS-95 model. The implementation in H2OI95 was instead compared with Table 8 of Helgeson and Kirkham (1974a), which presents compressibility values over a wide range of temperature (up to 900°C) and pressure (up to 8 kb, or 800 MPa). The Helgeson and Kirkham results were obtained from a different equation-of-state model (Keenan et al., 1969). The partial comparison shown in Table 5.1 is nevertheless reasonably good. H2OI95 calculations were made using test cases VCaks (saturation curve) and VCakx (specified pressures).

Table 5.1. Comparison of compressibility (κ_T, MPa^{-1}) calculated by H2OI95 with values given by Helgeson and Kirkham (1974a), hereafter HK74a. This is not an exact verification as different EOS models were used (see text).

		Saturation Pressure		100 MPa	
T(K)	T(C)	HK74a, Table 8	H2OI95	HK74a, Table 8	H2OI95
298.15	25	4.560×10^{-4}	4.526×10^{-4}	3.657×10^{-4}	3.572×10^{-4}
323.15	50	4.436×10^{-4}	4.418×10^{-4}	3.607×10^{-4}	3.483×10^{-4}
373.15	100	4.950×10^{-4}	4.902×10^{-4}	3.770×10^{-4}	3.697×10^{-4}
423.15	150	6.309×10^{-4}	6.204×10^{-4}	4.283×10^{-4}	4.290×10^{-4}
473.15	200	9.009×10^{-4}	8.832×10^{-4}	5.202×10^{-4}	5.295×10^{-4}
523.15	250	1.500×10^{-3}	1.465×10^{-3}	6.745×10^{-4}	6.893×10^{-4}
573.15	300	3.291×10^{-3}	3.198×10^{-3}	9.385×10^{-4}	9.464×10^{-4}
623.15	350	1.699×10^{-2}	1.679×10^{-2}	1.400×10^{-3}	1.374×10^{-3}
673.15	400			2.197×10^{-3}	2.115×10^{-3}
723.15	450			3.509×10^{-3}	3.408×10^{-3}
773.15	500			5.531×10^{-3}	5.443×10^{-3}
873.15	600			9.587×10^{-3}	9.452×10^{-3}
973.15	700			1.042×10^{-2}	1.041×10^{-2}
1073.15	800			1.022×10^{-2}	1.025×10^{-2}
1173.15	900			9.949×10^{-3}	1.002×10^{-2}

5.1.2. Isobaric Thermal Expansivity

The isobaric thermal expansivity is defined by:

$$\alpha_p = \frac{1}{v}\left(\frac{\partial v}{\partial T}\right)_p$$

This property has dimensions of inverse temperature. It can be shown that this is equivalent to

$$\alpha_p = -\frac{1}{\rho}\left(\frac{\partial \rho}{\partial T}\right)_p$$

Obtaining an expression for obtaining the expansivity from the equation-of-state model is more complicated than obtaining the one for the compressibility. There is a useful relation between the two properties (Helgeson and Kirkham, 1974a, equation (26)):

$$\left(\frac{\delta P}{\delta T}\right)_\rho = {\alpha_p}/{\kappa_T}$$

This is a kind of Maxwell relation, meaning that it ultimately relates to the equivalence of second order derivatives, regardless of order of differentiation.

It can then be shown that:

$$\alpha_p = -\left(\frac{\tau}{T}\right)\kappa_T\left(\frac{\partial p}{\partial \tau}\right)_\delta$$

The derivative here is analogous to the one needed to obtain the compressibility. Recall that

$$p = \rho RT(1 + \delta\phi_\delta^r)$$

Therefore

$$\frac{\partial p}{\partial \tau} = -\frac{p}{\tau} + {p\delta\phi_{\delta\tau}^r}\Big/{\left(1 + \delta\phi_\delta^r\right)}$$

No direct means were found to validate calculated results, in the sense that no tables were found that give thermal expansivity values calculated from the IAPWS-95 model. The implementation in H2OI95 was instead compared with Table 7 of Helgeson and Kirkham (1974a), which presents results over a wide range of temperature (25-900°C) and pressure (up to 8 kb, or 800 MPa). The Helgeson and Kirkham results were obtained from a different equation-of-state model (Keenan et al., 1969). The partial comparison shown in Table 5.2 is nevertheless good. H2OI95 calculations were made using test cases VCaks (saturation curve) and VCakx (specified pressures, but only results for 100 MPa are shown here).

Table 5.2. Comparison of thermal expansivity (a_v, K^{-1}) calculated by H2OI95 with values given by Helgeson and Kirkham (1974a), hereafter HK74a. This is not an exact verification as different EOS models were used (see text).

		Saturation Pressure		100 MPa	
T(K)	T(C)	HK74a, Table 7	H2OI95	HK74a, Table 7	H2OI95
298.15	25	2.553 x 10^{-4}	2.572 x 10^{-4}	3.430 x 10^{-4}	3.502 x 10^{-4}
323.15	50	4.624 x 10^{-4}	4.578 x 10^{-4}	4.576 x 10^{-4}	4.557 x 10^{-4}
373.15	100	7.486 x 10^{-4}	7.506 x 10^{-4}	6.303 x 10^{-4}	6.312 x 10^{-4}
423.15	150	1.027E-03	1.027E-03	7.951 x 10^{-4}	7.900 x 10^{-4}
473.15	200	1.376E-03	1.379E-03	9.560 x 10^{-4}	9.542 x 10^{-4}
523.15	250	1.951E-03	1.958E-03	1.127 x 10^{-3}	1.144 x 10^{-3}
573.15	300	3.295E-03	3.274E-03	1.354 x 10^{-3}	1.384 x 10^{-3}
623.15	350	1.038E-02	1.039E-02	1.692 x 10^{-3}	1.703 x 10^{-3}
673.15	400			2.163 x 10^{-3}	2.138 x 10^{-3}
723.15	450			2.721 x 10^{-3}	2.709 x 10^{-3}
773.15	500			3.274 x 10^{-3}	3.292 x 10^{-3}
873.15	600			3.310 x 10^{-3}	3.295 x 10^{-3}
973.15	700			2.369 x 10^{-3}	2.366 x 10^{-3}
1073.15	800			1.716 x 10^{-3}	1.716 x 10^{-3}
1173.15	900			1.332 x 10^{-3}	1.336 x 10^{-3}

5.1.3. The Dimensionless Isothermal Compressibility Function ζ

The dimensionless isothermal compressibility function is defined as

$$\zeta_T = \left(\frac{\partial \overline{\rho}}{\partial \overline{p}}\right)_T$$

(See Huber et al., 2009, and IAPWS, 2008, describing an IAPWS-sanctioned model for dynamic viscosity). Here $\overline{\rho} = \rho/\rho_{cr}$ and $\overline{p} = p/p_{cr}$. These are both dimensionless. Here $\overline{\rho} = \delta$ in the symbolism of the IAPWS-95 model (Wagner and Pruss, 2002; IAPWS, 2016). It follows from standard relations that

$$\zeta_T = p_{cr}\left(\frac{\partial\delta}{\partial p}\right)_T$$

and hence

$$\zeta_T = {p_{cr}}\Big/{\left(\frac{\partial p}{\partial\delta}\right)_T}$$

where the partial derivative is the same one used to obtain the compressibility κ_T. The two kinds of compressibility are related by

$$\zeta_T = p_{cr}\delta\kappa_T$$

The dimensionless isothermal compressibility is not addressed by Wagner and Pruss (2002), IAPWS (2016), or other common references addressing the thermophysical properties of water. However, ζ_T is used in models for the viscosity (Section 5.2.1) and thermal conductivity (Section 5.2.2), in particular in the "critical enhancement" part of those models, which describe corrections important mainly about the critical point. The descriptions of those models provide the only known available tests for computer verification of calculated values of ζ_T. See Section 5.2.1 for such verification.

.

5.2. Additional Properties Described by Supplementary Models

Other water properties cannot be derived solely from the equation-of-state model. Some of these, including dynamic viscosity and thermal conductivity, are properly considered transport properties. Some of the associated models require inputs that are most likely found using an EOS model, and models of this type tend to be developed using a specific EOS model. Such an input from an EOS model might be the relative density (δ) for a desired temperature and pressure. Calculating parts of the dynamic viscosity and the thermal conductivity requires the above described dimensionless isothermal compressibility function ζ_T. The specific models addressed here may be considered extensions or "add-ons" to the IAPWS-95 EOS model (Wagner and Pruss, 2002: IAWPS, 2016). They can also be applied

as extensions to the corresponding industrial formulation, IAPWS-IF97 (Wagner et al., 2000), or still other equation-of-state models, with some loss of accuracy.

Interest in these additional water properties was spurred by the discovery of coding of earlier models for these properties in SUPCRT92 (in the TRANS88 submodule in the H2O92D module, comprised of functions VISCOS, THCOND, and SURTEN, and subroutines BORN92, JN91, and EPSBRN). The relevant coding is executed in SUPCRT92, but the results do not seem to be output or used for any other purpose. These routines appear to be updates of corresponding routines from a previous version of SUPCRT. Some of these additional properties and corresponding models were used in the multi-year development of geochemical thermodynamic data and models intended for application over a wide range of temperature and pressure by H. C. Helgeson and colleagues (in particular see Helgeson and Kirkham, 1974a, 1974b, who used the Keenan et al., 1969 EOS model for water). The models in the TRANS88 subroutines in SUPCRT92 were intended for use with the Haar et al. (1984) equation-of-state model (IAP-84). It is thus apparent that the newer and currently sanctioned (IAPWS) models of such properties are of significance to ongoing and future thermodynamic database development.

5.2.1. Dynamic Viscosity

IAWPS (2008) describes the IAPWS-sanctioned model for the dynamic viscosity of water. The model is developed in the corresponding paper by Huber et al. (2009). The viscosity model found in SUPCRT92 is the much earlier one of Watson et al. (1980).

In the IAPWS (2008) model, the viscosity μ is given by

$$\mu = \mu^* \times \overline{\mu}$$

where $\mu^* = 1.00 \times 10^{-6}$ Pa-s. The dimensionless viscosity $\overline{\mu}$ is represented by:

$$\overline{\mu} = \overline{\mu}_0(\overline{T}) \times \overline{\mu}_1(\overline{T}, \overline{\rho}) \times \overline{\mu}_2(\overline{T}, \overline{\rho})$$

where $\overline{T} = T/T_{cr} = 1/\tau$ and $\overline{\rho} = \rho/\rho_{cr} = \delta$. The factor $\overline{\mu}_0$ is represented by a direct function of $\overline{T}$, and $\overline{\mu}_1$ is represented by a direct function of $\overline{T}$ and $\overline{\rho}$. These functions are, respectively, equations (11) and

(12) given by IAPWS (2008). The third factor, $\overline{\mu}_2$, is called the critical enhancement. It is only necessary in a small region of density and temperature space around the critical point.

IAPWS (2008) gives a moderately complex set of equations for calculating $\overline{\mu}_2$. This factor is a function of $\overline{T}$, $\overline{\rho}$, and the dimensionless isothermal compressibility function ζ_T discussed earlier. The need for a ζ_T input defines an interface between the viscosity model and an equation-of-state (EOS) model. In the IAPWS (2008) model, the development of the critical enhancement factor was made using ζ_T values obtained from IAPWS-95. Therefore, this viscosity model is most consistently used with this EOS model. According to IAPWS (2008), the viscosity model may also be used with the corresponding industrial formulation (IAPWS-IF97). It is suggested that when using the industrial formulation that the critical enhancement be neglected (effectively setting $\overline{\mu}_2$ to unity) for the sake of greater computational speed. The viscosity model could also be used with other EOS models, though with potential loss of accuracy.

The relevant equations and constants for the IAPWS (2008) model are given in the source document and the original paper by Huber et al. (2009) and will not be repeated here. The factor $\overline{\mu}_0$ is represented by an expression depending on $\overline{T}$. The factor $\overline{\mu}_1$ is given by an expression depending on $\overline{T}$ and $\overline{\rho}$. Lastly, the factor $\overline{\mu}_2$ is given by a set of expressions depending on $\overline{T}$, $\overline{\rho}$, ζ_T, and ζ_{T_R}, where T_R refers to a reference temperature of 1.5 × T_{cr}, or 970.644K. IAPWS (2008) offers no guidance on calculating ζ_{T_R}. The most accurate way is to use IAPWS-95 or an alternative EOS model. However, this requires a second evaluation of the EOS model for the model's reference temperature. For H2OI95, a function GZTTBR was created to evaluate ζ_{T_R} for the required density using three fourth-order polynomials, each for a difference density range. This was created by calculating ζ_{T_R} from the EOS model over the pressure range 0-1000 MPa and fitting polynomials to the calculated values as functions of dimensionless density. This polynomial treatment is not part of any IAPWS standard. Currently, H2OI95 uses the EOS model itself to obtain ζ_{T_R} values. This is more strictly accurate, though not as efficient.

IAPWS (2008) presents two tables for computer-program verification. The first is their Table 4, giving results obtained with $\overline{\mu}_2$ set to unity. This is intended to facilitate testing coding implementation of $\overline{\mu}_0$ and $\overline{\mu}_1$. As showin in Table 5.3, H2OI95 (test case VCvis, first part) reproduced these results exactly to the precision given by IAPWS (2008).

Table 5.3. Values of the dynamic viscosity (μPa-s) calculated with $\overline{\mu}_2 = 1$ (ignoring critical enhancement) comparing values given by IAPWS (2008, Table 4) with corresponding results from H2OI95. The comparison is exact to the precision given by IAPWS (2008, Table 4).

T(K)	ρ (kg-m^{-3})	IAPWS (2008, Table 4)	H2OI95
298.15	998	889.735100	889.735100
298.15	1200	1437.649467	1437.649467
373.15	1000	307.883622	307.883622
433.15	1	14.538324	14.538324
433.15	1000	217.685358	217.685358
873.15	1	32.619287	32.619287
873.15	100	35.802262	35.802262
873.15	600	77.430195	77.430195
1173.15	1	44.217245	44.217245
1173.15	100	47.640433	47.640433
1173.15	400	64.154608	64.154608

Table 5 of IAPWS (2008) is for testing coding implementation of the critical enhancement factor, $\overline{\mu}_2$. The temperature in all cases here is 647.35K, slightly above the critical temperature (647.096K). As noted in Appendix C, testing the implementation of the critical enhancement for viscosity in H2OI95 revealed a coding error of the IAPWS-95 EOS model in Version 1.0. This affected calculation of the dimensionless isothermal compressibility, mainly in a region around and close to the critical point.

The coding error was corrected in Version 1.1 of H2OI95. An on-line viscosity calculator (http://twt.mpei.ac.ru/mcs/worksheets/iapws/wspsDVRT.xmcd) at the Moscow Power Engineering Institute (MPEI) was helpful in tracking down the error. This calculator was created by the Russian National Committee (RNC) of the IAPWS. It gives intermediate results in the calculation of the dynamic viscosity, including values of the dimensionless isothermal compressibility.

Table 5.4 shows ζ_T values for the IAPWS (2008) Table 5 cases, comparing results obtained from the uncorrected H2OI95, the MPEI RNC IAPWS-95 calculator, and the corrected H2OI95. Results for the corrected H2OI95 are identical to the RNC IAPWS results to the number of significant figures shown. This constitutes verification of ζ_T values calculated in the corrected code (Version 1.1).

Table 5.4. Values of ζ_T for IAPWS (2008, Table 5) cases for computer-program verification in the region near the critical point. The temperature in all cases is 647.35K.

ρ (kg-m^{-3})	H2OI95 (version 1.0)	MPEI RNC Calculator*	H2OI95 (Version 1.1)
122	1.17236434	1.172359573	1.172359573
222	12.13628693	12.02261748	12.02261748
272	85.0003849	103.3499714	103.3499714
322	0.00000096**	831.6085703	831.6085703
372	56.57653032	85.37241366	85.37241366
422	9.25066217	8.93479199	8.934791993

*MPEI RNC IAWPS-95 on-line viscosity calculator:
http://twt.mpei.ac.ru/mcs/worksheets/iapws/wspsDVRT.xmcd.
**This value is effectively zero. It is obtained by resetting δ to a value just slightly different from unity in order to avoid a calculational singularity (see text).

For a density of 322 kg-m^{-3}, the IAPWS-95 model presents a numerical singularity [division by the quantity (δ - 1) when δ = 1] in the equation for the phi function $\phi^{\tau}_{\delta\delta}$, which is required to calculate $(\partial p/\partial\delta)_T$. That in turn is needed to obtain κ_T and ζ_T. The singularity is avoided by resetting δ to a value just slightly different from unity, such as 100 times the machine epsilon. The machine epsilon for 64-bit arithmetic on a Windows PC is about 2.2204 x 10^{-16}, hence 100 times that is about 2.2204 x 10^{-14}.

Table 5.5 shows critical enhancement ($\overline{\mu}_2$) values from IAPWS (2008) Table 5, compared with results obtained from the corrected H2OI95. When ζ_{T_R} values are obtained directly from the equation-of-state model, the H2OI95 results are identical to the IAPWS (2008) Table 5 values. A slight loss of accuracy is introduced when ζ_{T_R} values are instead estimated from the polynomial approximation in function GZTTBR.

Table 5.5. Values of the critical enhancement ($\overline{\mu}_2$) from IAPWS (2008, Table 5), compared with results obtained from the corrected version of H2OI95. The temperature in all cases is 647.35K.

ρ (kg-m^{-3})	IAPWS (2008, Table 5)	H2OI95 (Version 1.1)*	H2OI95 (Version 1.1)**
122	1.00000289	1.00000289	1.00000289
222	1.00375120	1.00375120	1.00375120
272	1.03416789	1.03416789	1.03416789
322	1.09190440	1.09190440	1.09190440
372	1.03665871	1.03665871	1.03665873
422	1.00596332	1.00596332	1.00596307

*Using ζ_{T_R} calculated from the IAPWS-95 model.
**Using ζ_{T_R} values calculated from fitted polynomials (function GZTTBR).

Table 5.6 compares dynamic viscosity values obtained from IAPWS (2008) Table 5, the MPEI RNC online calculator, and the corrected H2OI95. The corrected H2OI95 values agree perfectly with the MPEI RNC calculator values when all are rounded to the precision of the IAPWS (2008) Table 5 values. They match perfectly with the IAPWS (2208) Table 5 values except for the density of 422 kg-m^3, where the last digit is off by one.

As noted previously, H2OI95 Version 1.0 passed verification tests suggested by Wagner and Pruss (2002) and IAPWS (2016), as well as tests using the steam tables generated by Wagner and Pruss (2002). A test focusing on the dimensionless isothermal compressibility, focused on the region about the critical point, as in Table 5.4, appears to be needed for full verification of the implementation of IAPWS-95.

Table 5.6. Values of the dynamic viscosity (μPa-s) from IAPWS (2008, Table 5), compared with results obtained from the MPEI RNC Calculator and the corrected version of H2OI95. The temperature in all cases is 647.35K.

ρ (kg-m^{-3})	IAPWS (2008, Table 5)	MPEI RNC Calculator	H2OI95 (Version 1.1)*
122	25.520677	25.520677	25.520677
222	31.337589	31.337589	31.337589
272	36.228143	36.228143	36.228143
322	42.961579	42.961579	42.961579
372	45.688204	45.688204	45.688204
422	49.436257	49.436256	49.436256

*Using ζ_{T_R} calculated from the IAPWS-95 model.

The NIST on-line Chemistry WebBook entitled “Thermophysical Properties of Fluid Systems” (http://webbook.nist.gov/chemistry/fluid/) was used in earlier data comparisons in this report. However, it is not useful for viscosity comparisons because it uses an earlier (1985) IAPWS model.

5.2.2. Thermal Conductivity

IAPWS (2011) describes the IAPWS-sanctioned model for the thermal conductivity of water. The model is developed in the corresponding paper by Huber et al. (2012). The mathematical form of the thermal conductivity model somewhat follows that of the viscosity model described above, although it is not closely analogous.

The thermal conductivity λ is given by

$$\lambda = \lambda^* \times \overline{\lambda}$$

where $\lambda^* = 1.0 \times 10^{-3}$ W-K^{-1}-m^{-1}. The dimensionless thermal conductivity $\overline{\lambda}$ is represented by:

$$\overline{\lambda} = \overline{\lambda}_0(\overline{T}) \times \overline{\lambda}_1(\overline{T}, \overline{\rho}) + \overline{\lambda}_2(\overline{T}, \overline{\rho})$$

where $\overline{T} = T/T_{cr} = 1/\tau$ and $\overline{\rho} = \rho/\rho_{cr} = \delta$. The factor $\overline{\lambda}_0$ is represented by a direct function of $\overline{T}$, and $\overline{\lambda}_1$ by a direct function of $\overline{T}$ and $\overline{\rho}$. These functions are, respectively, equations (16) and (17) given by IAPWS (2011). The third factor, $\overline{\lambda}_2$, is the critical enhancement, analogous to that for the viscosity. However, note that the critical enhancement here is a term *added* to $\overline{\lambda}_0 \times \overline{\lambda}_1$, not an additional factor to be multiplied by them.

IAPWS (2011) give a set of equations for calculating $\overline{\lambda}_2$ that are somewhat more complex than those for calculating $\overline{\mu}_2$. This factor is a function of $\overline{T}$, $\overline{\rho}$, ζ_T, $\overline{\mu}$, c_p, and c_v. The need for ζ_T, c_p, and c_v input defines an interface between the thermal conductivity model and an equation-of-state (EOS) model. The need for $\overline{\mu}$ defines an interface with the viscosity model. In the IAPWS (2011) model, the development of the critical enhancement factor was made using values for these properties obtained from IAPWS-95 and IAPWS (2008). The thermal conductivity model is most consistently used with the IAPWS-95 model, though it may also be used with the corresponding industrial formulation (IAPWS-IF97). It is suggested that when using the industrial formulation that the critical enhancement be neglected (effectively setting $\overline{\lambda}_2$ to zero) for the sake of greater computational speed. The thermal conductivity model could also be used with other EOS models, though with potential loss of accuracy.

The full set of equations and constants for the IAPWS (2011) model are given in the source document and the original paper by Huber et al. (2012) and will not be repeated here. The factor $\overline{\lambda}_0$ is represented by an expression depending on $\overline{T}$. The factor $\overline{\lambda}_1$ is given by an expression depending on $\overline{T}$ and $\overline{\rho}$. Lastly, the factor $\overline{\lambda}_2$ is given by a set of expressions depending on $\overline{T}$, $\overline{\rho}$, ζ_T, $\overline{\mu}$, c_p, c_v, and ζ_{T_R}, where T_R again refers to a reference temperature of 1.5 × T_{cr}, or 940.644K. IAPWS (2011) offers no guidance in regard to calculating ζ_{T_R}. The most accurate way is again to use IAPWS-95 or an alternative EOS model, requiring a second evaluation of the EOS model for the reference temperature T_R. For H2OI95, the function

GZTTBR can again be used to estimate ζ_{T_R} using fourth-order polynomials. However, as in the case of calculating dynamic viscosity, H2OI95 currently uses the EOS model to obtain ζ_{T_R} values.

IAPWS (2011) presents two tables for computer-program verification. The first is their Table 4, giving results obtained with $\overline{\lambda}_2$ set to zero. This is intended to facilitate testing coding implementation of $\overline{\lambda}_0$ and $\overline{\lambda}_1$. H2OI95 (test case VCthc, first part) closely reproduced these results (Table 5.7).

Table 5.7. Values of the thermal conductivity (mW-m^{-1}-K^{-1}) calculated with $\overline{\lambda}_2 = 0$ (ignoring critical enhancement) comparing values given by IAPWS (2011, Table 4) with corresponding results from H2OI95. The comparison is exact or very nearly so to the precision given by IAPWS (2011, Table 4).

T(K)	ρ (kg-m^{-3})	IAPWS (2011, Table 4)	H2OI95
298.15	0	18.4341883	18.4341884
298.15	998	607.712868	607.712868
298.15	1200	799.038144	799.038144
873.15	0	79.1034659	79.1034659

Their second table (their Table 5) is for testing of the coding implementation of the critical enhancement factor, $\overline{\lambda}_2$. The temperature in all cases here is 647.35K, slightly above the critical temperature (647.096K). Comparison of results from H2OI95 (test case VCthc, second part) is shown in Table 5.8.

Table 5.8. Values of the critical enhancement ($\overline{\lambda}_2$) from IAPWS (2011, Table 5), compared with results obtained from H2OI95. The temperature in all cases is 647.35K. Comparison is exact to the number of significant figures given by IAPWS (2011). Comparison using the polynomial approximation for the dimensionless compressibility at the reference temperature shows small differences that are not of practical significance.

ρ (kg-m^{-3})	IAPWS (2011, Table 5)	H2OI95 (Version 1.1)*	H2OI95 (Version 1.1)**
1	0.0001300	0.0001300	0.0001297
122	20.3162320	20.3162320	20.3162435
222	188.091206	188.091206	188.091077
272	540.133176	540.133176	540.133148
322	1187.51354	1187.51354	1187.51358
372	356.53333	356.53333	356.53322
422	118.931062	118.931062	118.931914
750	3.3419303	3.3419303	3.3558582

*Using ζ_{T_R} calculated from the IAPWS-95 model.
**Using ζ_{T_R} values calculated from fitted polynomials (function GZTTBR).

Table 5.9 compares results obtained from the MPEI RNC calculator and the corrected H2OI95 with (complete) thermal conductivity values from IAPWS (2011) Table 5. The corrected H2OI95 values and the MPEI RNC calculator values, rounded to the precision of the IAPWS (2011) Table 5 values, agree perfectly with those values.

Table 5.9. Values of thermal conductivity (mW-m^{-1}-K^{-1}) from IAPWS (2011, Table 5), compared with results obtained from the MPEI RNC Calculator and the corrected version of H2OI95. The temperature in all cases is 647.35K.

ρ (kg-m^{-3})	IAPWS (2011, Table 5)	MPEI RNC Calculator*	H2OI95 (Version 1.1)**
1	51.9298924	51.9298924	51.9298924
122	130.922885	130.922885	130.922885
222	367.787459	367.787459	367.787459
272	757.959776	757.959776	757.959776
322	1443.75556	1443.75556	1443.75556
372	650.319402	650.319402	650.319402
422	448.883487	448.883487	448.883487
750	600.961346	600.961346	600.961346

*MPEI RNC IAWPS-95 on-line thermal conductivity calculator: http://twt.mpei.ac.ru/mcs/worksheets/iapws/wspsTCRT.xmcd.
**Using ζ_{T_R} calculated from the IAPWS-95 model.

5.2.3. Surface Tension

IAPWS (2014) describes the IAPWS-sanctioned model for the surface tension of water. The model is based on the work of Vargaftik et al. (1983). The model describes to the surface tension between coexisting vapor and liquid. The surface tension (σ) is treated as a simple function of temperature, covering the range from the triple-point temperature (273.316K) to the critical temperature (647.096K):

$$\sigma = B\tau^{\mu}(1 + b\tau)$$

where B, μ, and b are constants and

$$\tau = 1 - \frac{T}{T_{cr}}$$

Table 5.10 compares selected values of surface tension from IAPWS (2014, Table 1) with values calculated by H2OI95. The H2OI95 values match to the precision given by IAPWS (2014, Table 1).

Table 5.10. Selected values of surface tension (mN-m^{-1}) from IAPWS (2014, Table 1), compared with results obtained from H2OI95.

Temp. °C	Temp. K	IAPWS (2014, Table 1)	H2OI95
0.01	273.16	75.65	75.65
25	298.15	71.97	71.97
50	323.15	67.94	67.94
75	348.15	63.58	63.58
100	373.15	58.91	58.91
125	398.15	53.96	53.96
150	423.15	48.74	48.74
175	448.15	43.30	43.30
200	473.15	37.67	37.67
225	498.15	31.90	31.90
250	523.15	26.04	26.04
275	548.15	20.16	20.16
300	573.15	14.36	14.36
325	598.15	8.77	8.77
350	623.15	3.67	3.67
370	643.15	0.39	0.39
373.946	647.096	-----	0.00

5.2.4. Dielectric Constant

IAPWS (1997) describes the IAPWS-sanctioned model for the dielectric constant of water. The model is developed in the corresponding paper by Fernández et al. (1997). The dielectric constant is one of the most important properties of water, as it in turn is needed to calculate Born functions and Debye-Hückel parameters (Helgeson and Kirkham, 1974ab; Fernández et al., 1997). The IAPWS (1997) model treats the dielectric constant (ϵ) as a function of temperature and density. The relevant equations and constants for the model are given in the source document and the paper by Fernández et al. (1997) and will not be repeated here. It is noted that ρ in these documents refers to density mostly in units of mol-m^{-3}, not the usual kg-m^{-3}. In the model equations, density is referred to in units of mol-m^{-3}.

The dielectric constant, or relative permittivity (permittivity divided by the permittivity of free space), is dimensionless. Permittivity itself has dimensions of C^2-J^{-1}-m^{-1} (C referring to Coulombs). In the model, the permittivity of free space is given by an expression rather than a simple constant.

Values of the dielectric constant from IAPWS (1997, Table 4) intended for code verification are compared in Table 5.11 with corresponding results from H2OI95. Corresponding values match to the precision shown.

Table 5.11. Values of the dielectric constant (ϵ) from IAPWS (1997, Table 4), compared with results obtained from H2OI95.

p (MPa)	T (K)	IAPWS (1997)	H2OI95
0.101325	240	104.34982	104.34982
0.101325	300	77.74735	77.74735
10	300	78.11269	78.11269
1000	300	103.69632	103.69632
10	650	1.26715	1.26715
100	650	17.71733	17.71733
500	650	26.62132	26.62132
10	870	1.12721	1.12721
100	870	4.98281	4.98281
500	870	15.09746	15.09746

Other sources for potential comparison exist but were not used here. It is noted that an on-line dielectric constant calculator (http://twt.mpei.ac.ru/MCS/Worksheets/WSP/DIELEC97.xmcd) exists at the Moscow Power Engineering Institute (MPEI) created by the RNC of the IAPWS. This calculator uses temperature and density as inputs, not temperature and pressure.

IAPWS (2014) does not address partial derivatives (with respect to temperature and pressure) of the dielectric constant and various derivative properties, such as Debye-Hückel parameters and Born functions. However, the source paper by Fernández et al. (1997) addresses the first-order partial derivatives and the Debye-Hückel “A” (or limiting law) parameters.

Table 5.12 compares values of the temperature derivative given by Fernández et al. (1997) with values obtained from H2OI95. Table 5.13 shows a similar comparison for the pressure derivative. In both tables, the agreement is perfect to the precision given by Fernández et al. (1997).

Table 5.12. Values of the temperature derivative of the dielectric constant (ϵ) from Fernandez et al. (1997, Table 17), compared with results obtained from H2OI95.

	10 MPa		100 MPa		1000 MPa	
T (K)	Fernandez et al. (1997)	H2OI95	Fernandez et al. (1997)	H2OI95	Fernandez et al. (1997)	H2OI95
300	-0.357011	-0.357011	-0.367852	-0.367852	-0.481815	-0.481815
350	-0.284884	-0.284884	-0.286956	-0.286956	-0.334865	-0.334865
400	-0.227249	-0.227249	-0.225663	-0.225663	-0.251380	-0.251380
450	-0.183607	-0.183607	-0.178549	-0.178549	-0.195865	-0.195865
500	-0.153818	-0.153818	-0.143247	-0.143247	-0.154787	-0.154787
550	-0.139993	-0.139993	-0.117403	-0.117403	-0.123594	-0.123594
600			-0.0986724	-0.0986724	-0.0997915	-0.0997915
650			-0.0848987	-0.0848987	-0.0815521	-0.0815521
700			-0.0738557	-0.0738557	-0.0674716	-0.0674716
750			-0.0625236	-0.0625236	-0.0564897	-0.0564897
800			-0.0478270	-0.0478270	-0.0478210	-0.0478210

Table 5.13. Values of the pressure derivative of the dielectric constant (ϵ) from Fernandez et al. (1997, Table 17), compared with results obtained from H2OI95.

	10 MPa		100 MPa		1000 MPa	
T (K)	Fernandez et al. (1997)	H2OI95	Fernandez et al. (1997)	H2OI95	Fernandez et al. (1997)	H2OI95
300	0.0366343	0.0366343	0.0325748	0.0325748	0.0212872	0.0212872
350	0.0340834	0.0340834	0.0290383	0.0290383	0.0168932	0.0168932
400	0.0350839	0.0350839	0.0282478	0.0282478	0.0147872	0.0147872
450	0.0389336	0.0389336	0.0287410	0.0287410	0.0134011	0.0134011
500	0.0476630	0.0476630	0.0304254	0.0304254	0.0122648	0.0122648
550	0.0695410	0.0695410	0.0335966	0.0335966	0.0112878	0.0112878
600			0.0387450	0.0387450	0.0104519	0.0104519
650			0.0464881	0.0464881	0.00974377	0.00974377
700			0.0571346	0.0571346	0.00914626	0.00914626
750			0.0686834	0.0686834	0.00864069	0.00864069
800			0.0734450	0.0734450	0.00820919	0.00820919

5.2.5. Debye-Hückel Parameters

The Debye-Hückel parameters include the "A" or "limiting law" parameters and "B" or "extended" parameters. The primary A and B parameters (commonly given as A_γ and B_γ) are used in some form of the basic Debye-Hückel model for describing the activity coefficient of an aqueous electrolyte or ion in dilute solution, or as part of some more elaborate model for more concentrated solutions (such as Pitzer's 1973 equations). For an extended discussion of aqueous activity coefficient models, see Section 3 of Wolery, 1992 or any other pertinent review of the subject. Aqueous geochemistry texts such as Anderson (2005) and Walther (2009) include discussions of such models. Helgeson and Kirkham (1974b) provide a wide-ranging discussion of Debye-Hückel parameters and Born functions (which are also related to the partial derivatives of the dielectric constant).

The basic Debye-Hückel model can be written as:

$$\log \gamma_i = \frac{-A_{\gamma,10} z_i^2 \sqrt{I}}{1+\text{å}_i B_\gamma \sqrt{I}}$$

where γ_i is the activity coefficient of the *i*-th ion, z_i is the charge number of that ion, å_i is the ion's diameter (commonly the "ion size"), I is the ionic strength, $A_{\gamma,10}$ is explicitly the "A_γ" parameter for calculating the base ten logarithm of the activity coefficient, and B_γ is the relevant Debye-Hückel "B" parameter. An equivalent form is:

$$\ln \gamma_i = \frac{-A_{\gamma,e} z_i^2 \sqrt{I}}{1+\text{å}_i B_\gamma \sqrt{I}}$$

where $\ln \gamma_i$ is the natural logarithm of the activity coefficient and $A_{\gamma,e}$ is explicitly the "A_γ" parameter for calculating the natural logarithm of the activity coefficient. The $\mathring{a}$ parameter is somewhat problematic in that a thermodynamic inconsistency (in the Gibbs-Duhem equation or cross-differentiation [Maxwell] relation for the activity coefficients of two ions) results unless å_i is the same for all ions in solution. Some models used a fixed value in place of å_i or the product $\text{å}_i B_\gamma$. The latter practice is problematic because B_γ is a function of temperature and pressure, as is A_γ. Some models avoid å_i and B_γ by using a "limiting law" form such as:

$$\ln \gamma_i = -A_{\gamma,e} z_i^2 \sqrt{I}$$

In common usage, A_γ is just written as such, and the reader is expected to know from the context which form it is. The relation between the two A_γ parameters is commonly written as:

$$A_{\gamma,e} = 2.303\, A_{\gamma,10}$$

where "2.303" stands for ln(10), with the understanding that the value 2.303 is not quite sufficiently accurate for precise work.

Pitzer's (1973) equations use a different model for the limiting law that employs a different "A" parameter denoted as A_ϕ. It is related to the A_γ forms by:

$$A_\phi = \frac{A_{\gamma,e}}{3} = \frac{2.303\, A_{\gamma,10}}{3}$$

The Debye-Hückel "A" and "B" parameters are dependent on the dielectric constant, which depends on temperature and pressure. In addition to the constants noted above, there are others associated with related thermodynamic properties, for example A_V (with apparent molar volume), A_H (with apparent molar enthalpy), A_K (with apparent molar compressibility), and A_C (with apparent molar heat capacity). These are discussed by Fernandez et al. (1997) and Helgeson and Kirkham (1974b). Helgeson and Kirkham also discuss the corresponding "B" parameters.

For H2OI95 version 1.1, the calculated Debye-Hückel parameters include A_ϕ, $A_{\gamma,e}$, $A_{\gamma,10}$, A_V, A_H, B_γ, B_V, and B_H. A_H is tabulated as A_H/RT, and B_H as B_H/RT. The "A" and "B" parameters associated with compressibility and heat capacity are not currently treated, as they require second partial derivatives of the dielectric constant, functions which Fernandez et al. (1997) do not provide. Also, some would require higher-order "phi" functions (specifically $\phi'^{i}_{\delta\delta\delta}$, $\phi'^{i}_{\delta\delta\tau}$, $\phi'^{i}_{\delta\tau\tau}$, and $\phi'^{i}_{\tau\tau\tau}$) than are given as part of the IAPWS-95 EOS model. A significant effort would be required to develop all the requisite equations. Fernandez et al. (1997) suggest that if higher-order functions such as A_K and A_C are desired, one might utilize numerical differentiation. They include examples of this approach. Although they do not explicitly say this, their tone seems to suggest that a better model for the dielectric constant might be desirable if one were to seriously address the higher-order parameters.

Fernandez et al. (1997) give the requisite equations for the "A" parameters considered here. These have been coded in subroutine DIELEC of H2OI95. Table 5.14 compares values of A_ϕ ($kg^{1/2}$ $mol^{-1/2}$) from Fernandez et al. (1977, Table 17) with values calculated using H2OI95. Results match to the precision given by Fernandez et al. It is apparent that similar closeness would be attained for $A_{\gamma,e}$ and $A_{\gamma,10}$, hence no comparisons for those parameters are presented here.

Table 5.14. Values of the Debye-Hückel limiting law parameter A_φ ($kg^{1/2}$ $mol^{-1/2}$) from Fernandez et al. (1997, Table 17), compared with results obtained from H2OI95.

	10 MPa		100 MPa		1000 MPa	
T (K)	Fernandez et al. (1997)	H2OI95	Fernandez et al. (1997)	H2OI95	Fernandez et al. (1997)	H2OI95
300	0.39062	0.39062	0.37505	0.37505	0.28396	0.28396
350	0.43196	0.43196	0.41139	0.41139	0.30807	0.30807
400	0.48972	0.48972	0.45996	0.45996	0.33202	0.33202
450	0.56654	0.56654	0.52081	0.52081	0.35814	0.35814
500	0.67109	0.67109	0.59528	0.59528	0.38630	0.38630
550	0.83030	0.83030	0.68741	0.68741	0.41568	0.41568
600			0.80562	0.80562	0.44557	0.44557
650			0.96577	0.96577	0.47552	0.47552
700			1.1969	1.1969	0.50527	0.50527
750			1.5472	1.5472	0.53474	0.53474
800			2.0669	2.0669	0.56392	0.56392

Table 5.15 compares values of A_V (cm^3 $kg^{1/2}$ $mol^{-3/2}$) from Fernandez et al. (1977, Table 17) with values calculated using H2OI95. Results match closely to the precision given by Fernandez et al. (some minor differences are apparent).

Table 5.16 compares values of A_H/RT ($kg^{1/2}$ $mol^{-1/2}$) from Fernandez et al. (1977, Table 17) with values calculated using H2OI95. Results match to the precision given by Fernandez et al.

Table 5.17 compares values for $A_{\gamma,10}$ ($kg^{1/2}$ $mol^{-1/2}$) reported by Helgeson and Kirkham (1974b), hereafter HK74b, with ones obtained from H2OI95. The comparison is fair to good. Helgeson and Kirkham used a different model for the dielectric constant (their own) and a different EOS model for water (Keenan et al., 1969). Thus, small differences are to be expected.

Table 5.15. Values of the Debye-Hückel parameter A_V ($cm^3\ kg^{1/2}\ mol^{-3/2}$) from Fernandez et al. (1997, Table 17), compared with results obtained from H2OI95.

	10 MPa		100 MPa		1000 MPa	
T (K)	Fernandez et al. (1997)	H2OI95	Fernandez et al. (1997)	H2OI95	Fernandez et al. (1997)	H2OI95
300	1.8857	1.8857	1.5854	1.5854	0.70218	0.70217
350	3.0191	3.0191	2.3625	2.3624	0.86445	0.86444
400	5.2234	5.2234	3.7522	3.7521	1.1319	1.1319
450	9.6718	9.6716	6.1132	6.1131	1.4923	1.4923
500	20.023	20.022	10.230	10.229	1.9331	1.9330
550	52.399	52.398	17.800	17.800	2.4520	2.4519
600			32.686	32.686	3.0526	3.0526
650			64.214	64.213	3.7421	3.7420
700			135.69	135.69	4.5293	4.5292
750			299.47	299.47	5.4244	5.4243
800			616.62	616.61	6.4374	6.4373

Table 5.16. Values of the Debye-Hückel parameter A_H/RT ($kg^{1/2}\ mol^{-1/2}$) from Fernandez et al. (1997, Table 17), compared with results obtained from H2OI95.

	10 MPa		100 MPa		1000 MPa	
T (K)	Fernandez et al. (1997)	H2OI95	Fernandez et al. (1997)	H2OI95	Fernandez et al. (1997)	H2OI95
300	0.80315	0.80315	0.72666	0.72666	0.60001	0.60001
350	1.3821	1.3821	1.1891	1.1891	0.65507	0.65507
400	2.1291	2.1291	1.7485	1.7485	0.79737	0.79737
450	3.1823	3.1823	2.4212	2.4212	0.98133	0.98133
500	4.9811	4.9811	3.2934	3.2934	1.1563	1.1563
550	9.1593	9.1593	4.5447	4.5447	1.3084	1.3084
600			6.5128	6.5128	1.4388	1.4388
650			9.8437	9.8437	1.5534	1.5534
700			15.739	15.739	1.6584	1.6584
750			25.776	25.776	1.7591	1.7591
800			38.835	38.835	1.8592	1.8592

Table 5.17. Values of the Debye-Hückel limiting law parameter $A_{\gamma,10}$ ($kg^{1/2}$ $mol^{-1/2}$) from Helgeson and Kirkham (1974b) [HK74b] compared with results obtained from H2OI95.

	Saturation Curve		100 MPa (1 kbar)		500 MPa (5 kbar)	
T (C)	HK74b, Table 1	H2OI95	HK74b, Table 1	H2OI95	HK74b, Table 1	H2OI95
25	0.5092	0.5098	0.4882	0.4872	0.4417	0.4231
50	0.5336	0.5341	0.5096	0.5086	0.457	0.4402
75	0.5639	0.5638	0.5353	0.5340	0.4748	0.4585
100	0.5998	0.5990	0.5649	0.5633	0.4947	0.4782
150	0.6898	0.6871	0.6352	0.6339	0.5387	0.5227
200	0.8099	0.8051	0.7196	0.7210	0.5863	0.5729
250	0.9785	0.9716	0.8192	0.8278	0.6366	0.6275
300	1.2555	1.2421	0.9398	0.9617	0.6905	0.6856
350	1.9252	1.8878	1.0981	1.1377	0.7513	0.7465
400			1.3262	1.3830	0.8225	0.8101
450			1.6723	1.7467	0.9049	0.8767
500			2.1872	2.3002	0.9889	0.9465
550			2.8476	3.0790	1.0428	1.0197
600			3.3281	3.9891	1.0081	1.0966

Fernandez et al. (1997) do not address the Debye-Hückel "B" functions. Equations for calculating B_γ (cm^{-1} $kg^{1/2}$ $mol^{-1/2}$) and the broader set of "B" parameters are given by Helgeson and Kirkham (1974b). B_γ is tied to the "ion size" parameter å through the product åB_γ. The ion size parameter is generally specified in Angstroms (1 Å = 10^{-8} cm). Thus, tabulations of B_γ are commonly made in units of $kg^{1/2}$ $mol^{-1/2}$ $Å^{-1}$. Alternatively, they are given in units of $kg^{1/2}$ $mol^{-1/2}$ cm^{-1}, with the value shown being multiplied by 10^8. In the header of their Table 2, Helgeson and Kirkham (1974b) refer to tabulated B_γ in cm^{-1} $kg^{1/2}$ $mol^{-1/2}$ "x 10^{-8}". They mean, take the tabulated value and multiply it by 10^{-8}. This sort of language for dealing with powers of ten is at best ambiguous in the sense that different readers may take opposing meanings regarding the sign of the exponent (never mind the technical logic).

Helgeson and Kirkham use similar power of ten multipliers for other tabulated "B" and other types of functions. Accounting for their "sign convention," Helgeson and Kirkham give incorrect multipliers for B_V and B_H (and likely also for other parameters that will not be addressed here). This was discovered by numerical differentiation of Helgeson and Kirkham's tabulated data for B_γ with respect to temperature and

pressure and application of the requisite equations for B_V and B_H (their equations 49 and 8, respectively). Values of B_γ are not uncommon in the aqueous geochemistry literature (see for example Anderson, 2005, or Walther, 2009), at least for low temperature. Thus, there is no uncertainty regarding powers-of-ten for this parameter. The need for power of ten multipliers is reduced or eliminated if values of "B" parameters are given in terms of "$Å^{-1}$" to account for å being in units of Angstroms.

Table 5.18 compares values for B_γ ($Å^{-1}$ $kg^{1/2}$ $mol^{-1/2}$) reported by Helgeson and Kirkham (1974b) (hereafter HK74b in the following tables) with results obtained from H2OI95. The comparison is again generally good. Again, Helgeson and Kirkham used different models to obtain their results.

Table 5.18 Values of the Debye-Hückel parameter B_γ ($Å^{-1}$ $kg^{1/2}$ $mol^{-1/2}$) from Helgeson and Kirkham (1974b) [HK74b], compared with results obtained from H2OI95.

	Saturation Curve		100 MPa (1 kbar)		500 MPa (5 kbar)	
T (C)	HK74b, Table 2	H2OI95	HK74b, Table 2	H2OI95	HK74b, Table 2	H2OI95
25	0.3283	0.3284	0.3281	0.3279	0.3280	0.3236
50	0.3325	0.3326	0.3317	0.3315	0.3304	0.3267
75	0.3371	0.3371	0.3358	0.3355	0.3334	0.3299
100	0.3422	0.3420	0.3402	0.3399	0.3366	0.3333
150	0.3533	0.3528	0.3496	0.3493	0.3435	0.3405
200	0.3655	0.3647	0.3592	0.3594	0.3503	0.3480
250	0.3792	0.3782	0.3686	0.3698	0.3567	0.3553
300	0.3965	0.3950	0.3780	0.3807	0.3629	0.3623
350	0.4256	0.4229	0.3882	0.3925	0.3694	0.3688
400			0.4004	0.4057	0.3766	0.3749
450			0.4154	0.4213	0.3843	0.3805
500			0.4321	0.4392	0.3912	0.3858
550			0.4454	0.4569	0.3934	0.3907
600			0.4428	0.4703	0.3842	0.3954

Table 5.19 compares values of B_V (cm^3 $kg^{1/2}$ $mol^{-3/2}$ $Å^{-1}$) from Helgeson and Kirkham (1974b) compared with results obtained from H2OI95. The Helgeson and Kirkham results are for "x 10^{-6}" corrected to "x 10^{-10}" and for a change in units. Results match reasonably well, at least for lower temperatures.

Differences are again a consequence of the usage of different EOS models and different models for the dielectric constant.

Table 5.19. Values of the Debye-Hückel parameter B_V ($cm^3\ kg^{1/2}\ mol^{-3/2}\ Å^{-1}$) from Helgeson and Kirkham (1974b) [HK74b], compared with results obtained from H2OI95.

	Saturation Curve		100 MPa (1 kbar)		500 MPa (5 kbar)	
T (C)	HK74b, Table 12	H2OI95	HK74b, Table 12	H2OI95	HK74b, Table 12	H2OI95
25	-0.0207	-0.0458	---	-0.0812	---	-0.1450
50	-0.1032	-0.1341	-0.0816	-0.1370	-0.0113	-0.1547
75	-0.2047	-0.2309	-0.1534	-0.2028	-0.0354	-0.1767
100	-0.3392	-0.3467	-0.2399	-0.2809	-0.0611	-0.2086
150	-0.7761	-0.6794	-0.4768	-0.4829	-0.1154	-0.2915
200	-1.6521	-1.2943	-0.8402	-0.7768	-0.1668	-0.3912
250	-3.6691	-2.6954	-1.4098	-1.2341	-0.2043	-0.5053
300	-9.8409	-7.1878	-2.3424	-1.9970	-0.2168	-0.6358
350	-53.3698	-45.0155	-3.945	-3.3473	-0.1976	-0.7868
400			-6.6802	-5.8327	-0.1485	-0.9629
450			-10.9055	-10.3317	-0.0878	-1.1682
500			-16.1273	-17.1020	-0.0573	-1.4055
550			-19.2425	-22.7126	-0.1185	-1.6759
600			-16.5262	-22.0764	-0.2937	-1.9779

Table 5.20 compares values of B_H/RT ($kg^{1/2}\ mol^{-1/2}\ Å^{-1}$) from Helgeson and Kirkham (1974b) with values from H2OI95. The Helgeson and Kirkham results are for "x 10^{-9}" corrected to "x 10^{-7}" and for a change in units. Again, results match reasonably well, at least for lower temperatures.

The set of Debye-Hückel parameters addressed here in H2OI95 should be sufficient for most problems likely to be encountered in aqueous geochemistry. Indeed, the present set generally exceeds what is found on most thermodynamic databases that directly support many existing thermodynamic and reactive transport modeling codes. As geochemical interest moves deeper into the earth and increasingly extends to planetology, an expanded set of parameters as well as newer, more expansive models may become necessary. Therefore, what is presented here is only a good start.

Table 5.20. Values of the Debye-Hückel limiting law parameter B_H/RT ($kg^{1/2}$ $mol^{-1/2}$ $Å^{-1}$) from Helgeson and Kirkham (1974b) [HK74b], compared with results obtained from H2OI95.

	Saturation Curve		100 MPa (1 kbar)		500 MPa (5 kbar)	
T (C)	HK74b, Table 4	H2OI95	HK74b, Table 4	H2OI95	HK74b, Table 4	H2OI95
25	0.2127	0.2176	0.1823	0.1870	0.1181	0.1677
50	0.2630	0.2579	0.2305	0.2272	0.1635	0.1867
75	0.3129	0.3036	0.2732	0.2695	0.2009	0.2105
100	0.3610	0.3503	0.3115	0.3105	0.2306	0.2378
150	0.4551	0.4436	0.3722	0.3835	0.2700	0.2889
200	0.5632	0.5521	0.4148	0.4467	0.2882	0.3250
250	0.7493	0.7283	0.4502	0.5112	0.3020	0.3460
300	1.2436	1.1557	0.5084	0.5928	0.3319	0.3563
350	3.8160	3.5799	0.6323	0.7111	0.3892	0.3605
400			0.8403	0.8867	0.4680	0.3621
450			1.0800	1.1215	0.5136	0.3630
500			1.1670	1.3172	0.3853	0.3643
550			0.6230	1.2326	-0.1700	0.3659
600			-1.3480	0.8159	-1.3959	0.3674

5.2.6. Melting Pressure and Melting Temperature

The previously described models for the viscosity (IAPWS R12-08, 2008) and thermal conductivity (IAPWS R15-11, 2011) have temperature ranges of validity partially defined in terms of the melting temperature as a function of pressure. The model for the melting temperature is taken from IAPWS (R14-08, 2011), which in turn is based on the paper of Wagner et al. (2011). This model describes the melting pressure as a function of temperature.

To obtain the melting temperature as a function of pressure, it is necessary to invert the model. In H2OI95, the model for the melting pressure is implemented in function PMELT. The inversion is accomplished in function TKMELT using a secant method iteration. Iteration to find the melting temperature is illustrated by the following snippet of output:

```
 Temp(K)         press(MPa)
 647.3500        0.221318931E+02

TKMELT: iter=  0, tmelt= 251.165000000K, residual= 186.431263110 MPa
TKMELT: iter=  1, tmelt= 270.826035693K, residual= 7.454434884 MPa
TKMELT: iter=  2, tmelt= 271.414102744K, residual= 0.314425767 MPa
TKMELT: iter=  3, tmelt= 271.439999551K, residual= -0.004427130 MPa
TKMELT: iter=  4, tmelt= 271.439639985K, residual= 0.000002637 MPa
TKMELT: iter=  5, tmelt= 271.439640199K, residual= 0.000000000 MPa
```

6. Concluding Remarks

The IAPWS-95 model (Wagner and Pruss, 2002) slightly modified by IAPWS (2016) has been implemented in the program H2OI95. The program is written in simple Fortran and can be used as a basis for incorporating the IAPWS-95 model into codes such as SUPCRT92 (Johnson et al., 1992), which calculates the thermodynamic and thermochemical properties of chemical species including water over a wide range of temperature and pressure. H2OI95 calibrates the thermochemical properties to match the recommended CODATA key values (Cox et al., 1989). The implementation has been carefully validated against results given by both IAPWS (2016) and Wagner and Pruss (2002). The software is provided as both a Windows PC executable and source code. The present user interface is handled through a text-based input file, and output includes a text-based output file and three .csv (comma-separated-variable) files that can be opened by a spreadsheet or plotting program. A test case library is included as part of the package. The simple Fortran source code could be easily translated into another programming language such as C/C++ or Visual Basic.

The IAPWS-95 model, like previous equation-of-state models for water, is mathematically complex and exhibits very complex ("non-cubic") behavior below the critical temperature. The model uses inverse reduced temperature and reduced density as its primary variables. Thus, for common problems of specified pressure and temperature, specified temperature at saturation pressure, and specified pressure at saturation temperature, iteration is required to find the density matching the desired pressure. This is done using Newton-Raphson iteration. The difficulty is that below the critical temperature, there may be multiple numerical solutions, of which only one can be valid (or two, on the saturation curve). The numerical solution found is a function of the starting estimate for the density (or densities, for problems involving the saturation curve). Some numerical solutions can be shown to be physically invalid, such as those have a negative derivative of pressure with respect to density ("unstable" solutions) or non-physical results for a physical property such as the square of the speed of sound, the heat capacity at constant pressure, or the absolute entropy. H2OI95 and other implementations of this and similar equation-of-state

models for water use default starting values that are thought to generally lead to valid results. However, neither Wagner and Pruss (2002) nor IAPWS (2016) address the issue of starting estimates and multiple numerical solutions. H2OI95 has been used to conduct numerical studies of the IAPWS-95 model to complement those made by Junglas (2008). Results of these numerical studies have been used to identify default density values that lead to valid results for problems with specified temperature and pressure.

During testing it was found that for problems with specified temperature and pressure, there are convergence issues between the triple point temperature (273.16K) and 298.15K and between 647.082K and the critical point temperature (647.096K). It was necessary to apply looser convergence criteria in these temperature ranges. Others including Junglas (2008) and Haar et al. (1984, for the earlier IAPS-84 equation of state model) used similar accommodations, and it is likely that this is also the case for other water equation-of-state solvers. Junglas (2008) ascribed the need for such accommodations to the highly non-cubic behavior of the IAPWS-95 model in these regions, but there is more to it. The model itself is not consistent with true convergence in these regions, but only nearly so. The signed residual function never reaches the zero line, but only gets very close. A "solution" thus exists only for some minimum tolerance, not an arbitrarily small tolerance consistent with the 64-bit machine epsilon (smallest positive floating point number). The model is challenged in these circumstances, but the results are still satisfactory from a practical perspective. It is possible that some other set of model equations might avoid this problem, and this would represent at least a small improvement over the IAPWS-95 model.

Additional numerical studies are recommended if one is attempting to extrapolate the IAPWS-95 model outside its specified range of temperature and pressure. The user should remain cognizant that the model equations are complex with limited basis in theory, and that the model itself was fit to data only within the specified range of temperature and pressure.

Version 1.1 of H2OI95 extends the range of calculated water properties and parameters. It calculates some properties (e.g., isobaric thermal expansivity and isothermal compressibility) obtainable from the IAPWS-95 model but for which equations are not given by Wagner and Pruss (2002) or IAPWS (2016). It also calculates additional properties using supplementary or "add-on" models sanctioned by IAPWS. These include models for dynamic viscosity, thermal conductivity, surface tension, and static dielectric constant. The dielectric constant results are used to further calculate a limited set of Debye-Hückel parameters. In testing the implementation of the viscosity model, a coding error in the EOS model was found that mainly affects "higher-order" parameters such as the isothermal compressibility and the

dimensionless isothermal compressibility and then principally in a close vicinity of the critical point. The coding error (described in Appendix C) is corrected in Version 1.1.

Version 1.1 does not calculate values for all possible water properties obtainable from the EOS model (IAPWS-95). Additional properties would include the fugacity, the fugacity coefficient, and the compressibility factor Z. Also, this version does not calculate all possible properties based on the dielectric constant model, including some Debye-Hückel parameters and the entire set of Born functions (for discussion of such properties, see Helgeson and Kirkham (1974b). If one were to pursue calculations of these parameters, it might be desirable to pursue a better model for the dielectric constant itself (See Sverjensky et al., 2014).

Acknowledgments

This work was supported by the Spent Fuel and Waste Science and Technology (SFWST) program operated by the U.S. Department of Energy. The author thanks Carlos Jove-Colon of Sandia National Laboratories for many useful discussions during the conduct of this work.

References

Anderson G. (2005) *Thermodynamics of Natural Systems*, Second Edition. Cambridge University Press, New York. 648 pp. ISBN-13 978-0-521-84772-8.

Cox J. D., Wagman D. D., and Medvedev V. A., eds. (1989) *CODATA Key Values for Thermodynamics*. CODATA Series on Thermodynamic Values. Hemisphere Publishing Corp., New York. 271 pp. ISBN 0-89116-758-7.

Dick J. M. (2019) CHNOSZ: Thermodynamic calculations and diagrams for geochemistry. *Front. Earth Sci.* **7** (Article 180), 1-18.

Fernández D. P., Goodwin A. R. H., Lemmon, E. W., Levelt Sengers J. M. H., and Williams R. C. (2009) A formulation for the static permittivity of water and steam at temperatures from 238 k to 873 K at pressures up to 1200 MPa, including derivatives and Debye–Hückel coefficients. *J. Phys. Chem. Ref. Data* **26**, 1125-1166.

Grenthe I., Fuger J., Konings R. J. M., Lemire R. J., Muller A. B., Nguyen-Trung C., and Wanner, H. (1992) *Chemical Thermodynamics of Uranium*. Chemical Thermodynamics. Volume 1. North Holland Elsevier Science Publishers B. V., Amsterdam, The Netherlands. 715 pp.

Haar L., Gallagher J. S., and Kell G. S. (1984) *NBS/NRC Steam Tables*. Hemisphere Publishing Corporation, Washington, DC. 320 pp. ISBN 0-89116-353-0.

Am. J. Sci. Special Issues (free downloads of papers by Helgeson and co-authors, Parts I-IV noted below).

Helgeson H. C. and Kirkham, D. H. (1974a) Theoretical prediction of the thermodynamic behavior of aqueous electrolytes at high pressures and temperatures: I. Summary of the thermodynamic/electrostatic properties of the solvent. *Am. J. Sci.* **274**, 1089-1198.

Helgeson H. C. and Kirkham, D. H. (1974b) Theoretical prediction of the thermodynamic behavior of aqueous electrolytes at high pressures and temperatures: II. Debye-Hiickel parameters for activity coefficients and relative partial molal properties. *Am. Jour. Sci.* **274**, 1199-1261.

Helgeson H. C. and Kirkham, D. H. (1976) Theoretical prediction of the thermodynamic behavior of aqueous electrolytes at high pressures and temperatures: III. Equation of state for aqueous species at infinite dilution. *Am. Jour. Sci.* **276**, 97-240.

Helgeson H. C., Kirkham D. H., and Flowers G. C. (1981) Theoretical prediction of the thermodynamic behavior of aqueous electrolytes at high pressures and temperatures: IV. Calculation of activity coefficients, osmotic coefficients, and apparent molal and standard and relative partial molal properties to 600°C and 5 kb. *Am. Jour. Sci.* **281**, 1249-1546.

Holland T. J. B. and Powell R. (2011) An improved and extended consistent thermodynamic dataset for phases of petrological interest, involving a new equation of state for solids. *J. Meta. Geol.* **29**, 333-383.

Huber M. L., Perkins R. A., Laesecke A., Friend D. G., Sengers J. V., Assael M. J., Metaxa I. N., Vogel N. E., Mareš R., and Miyagawa K. (2009) New international formulation for the viscosity of H_2O. *J. Phys. Chem. Ref. Data* **38**, 101-125.

Huber M. L., Perkins R. A., Friend D. G., Sengers J. V., Assael M.J., Metaxa I. N., Miyagawa K., Hellmann R., and Vogel E. (2012) New international formulation for the thermal conductivity of H_2O. *J. Phys. Chem. Ref. Data* **41**, 033102, 1-23.

International Association for the Properties of Water and Steam, IAPWS R8-97 (1997), Release on the Static Dielectric Constant of Ordinary Water Substance for Temperatures from 238 K to 873 K and Pressures up to 1000 MPa (1997), 9 pp.

International Association for the Properties of Water and Steam, IAPWS R12-08 (2008), Release on the IAPWS Formulation 2008 for the Viscosity of Ordinary Water Substance (2008), 9 pp.

International Association for the Properties of Water and Steam, IAPWS R14-08 (2011), Revised Release on the Pressure along the Melting and Sublimation Curves of Ordinary Water Substance (2011), 7 pp.

International Association for the Properties of Water and Steam, IAPWS R15-11 (2011), Release on the IAPWS Formulation 2011 for the Thermal Conductivity of Ordinary Water Substance (2011), 15 pp.

International Association for the Properties of Water and Steam, IAPWS R1-76 (2014), Revised Release on Surface Tension of Ordinary Water Substance (2014), 6 pp.

International Association for the Properties of Water and Steam, IAPWS R6-95(2016), Revised Release on the IAPWS Formulation 1995 for the Thermodynamic Properties of Ordinary Water Substance for General and Scientific Use (2016), 19 pp. Note: the 2016 version has been replaced on the IAPWS web site (www.iapws.org) by the 2018 version.

International Association for the Properties of Water and Steam, IAPWS R6-95(2018), Revised Release on the IAPWS Formulation 1995 for the Thermodynamic Properties of Ordinary Water Substance for General and Scientific Use (2018), 19 pp.

Johnson J. W., Oelkers E. H., and Helgeson H. C. (1992) SUPCRT92: A software package for calculating the standard molal thermodynamic properties of minerals, gases, aqueous species, and reactions from 1 to 5000 bar and 0 to 1000°C. *Comp. Geosci.* **18**, 899-947.

Junglas P. (2008) Implementing the IAPWS-95 standard in MATLAB. Preprint – ICPWS XV, Berlin, September 8–11, 2008.

Keenan J. H., Keyes F. G., Hill P. G., and Moore J. G. (1969) *Steam Tables*. John Wiley & Sons, New York. 162 pp. ISBN-10: 0471465011.

Kiselev S. B. and Friend D. G. (1999) Revision of a multiparameter equation of state to improve the representation in the critical region: application to water. *Fluid Ph. Equilibria* **155**, 33-55.

Levelt Sengers J. M. H., Kamgar-Parsi, B., Balfour F. W., and Sengers J. V. (1983) Thermodynamic properties of steam in the critical region. *J. Phys. Chem. Ref. Data* 12, 1-28.

Miron G. D., Wagner T., Kulik D. A., and Lothenbach B. (2017) An internally consistent thermodynamic dataset for aqueous species in the system Ca-Mg-Na–K–Al–Si–O–C-H–Cl. *Am. J. Sci.* **317**, 754-805.

Shi L. and Mao S. (2012) Applications of the IAPWS-95 formulation in fluid inclusion and mineral-fluid phase equilibria. *Geosci. Front.* **3**, 51-58.

Sverjensky D. A., Harrison B., and Azzolini D. (2014). Water in the deep Earth: the dielectric constant and the solubilities of quartz and corundum to 60 kb and 1200 °C. *Geochim. Cosmochim. Acta* **129**, 125–145.

Vargaftik N. B., Volkov B. N., and Voljak L. D. (1983) International tables of the surface tension of water. *J. Phys. Chem. Ref. Data* **12**, 817-820.

Wagner W. and Pruss A. (2002) The IAPWS formulation 1995 for the thermodynamic properties of ordinary water substance for general and scientific use. *J. Phys. Chem. Ref. Data* **31**, 387-535.

Wagner W., Cooper J. R., Dittmann A., Kijima J., Kretzschmar H.-J., Kruse A., Mareš R., Oguchi K., Sato H., Stöcker I., Šifner O., Takaishi Y., Tanishita I., Trübenbach J., and Willkommen T. (2000) The IAPWS Industrial Formulation 1997 for the Thermodynamic Properties of Water and Steam. *J. Eng. Gas Turbines Power* **122**, 150-184.

Wagner W, Riethmann T., Feistel R., and Harvey A. H. (2001) New Equations for the Sublimation Pressure and Melting Pressure of H_2O Ice Ih. *J. Phys. Chem. Ref. Data* **40**, 043103, 1-11.

Walther J. V. (2009) *Essentials of Geochemistry*, second edition. Jones and Bartlett Publishers, LLC, Boston. 797 pp. ISBN: 978-0-7637-5922-3.

Watson J. T. R., Basu R. S., and Sengers J. V. (1980) An improved representative equation for the dynamic viscosity of water substance. *J. Phys. Chem. Ref. Data* **9**, 1255-1290.

Wilhelmsen Ø, Aasen A., Skaugen G., Aursand P., Austegard A, Aursand E., Gjennestad M. Aa., Lund H., Linga G., and Hammer M. (2017) Thermodynamic modeling with equations of state: Present challenges with established methods. *Ind. Eng. Chem. Res.* **56**, 3503-3515.

Wolery T. J. (1992) EQ3NR, A Computer Program for Geochemical Aqueous Speciation-Solubility Calculations: Theoretical Manual, User's Guide, and Related Documentation (Version 7.0). UCRL-MA-110662 PT III, Lawrence Livermore National Laboratory, Livermore, CA, 246 pp.

Zimmer K., Zhang Y., Lu P., Chen Y., Zhang G., Dalkilic M., and Zhu (2016) SUPCRTBL: A revised and extended thermodynamic dataset and software package of SUPCRT92. *Computers & Geosciences* **90** (Part A), 97-111.

Appendix A. Equations for Obtaining Thermochemical Results

Results obtained directly from the equation-of-state model (IAPWS-95 and similar models) are typically not consistent with standard thermochemical conventions, including those of CODATA (Cox et al., 1989). Helgeson and Kirkham (1974a) developed a translation approach to obtain thermochemical data for water in the original SUPCRT program noted earlier in this report. This program used the now outdated Keenan et al. (1969) equation-of-state model. A more straightforward translation approach is presented here. In the following discussion, lower case symbols denote quantities defined on a mass basis (e.g., units of J g^{-1} or J g^{-1} K^{-1}). Upper case symbols denote quantities defined on a molar basis (e.g., units of J mol^{-1} or J mol^{-1} K^{-1}). Symbols including the "°" sign (S°, $\Delta_f U°$, $\Delta_f H°$, $\Delta_f A°$, $\Delta_f G°$) denote quantities defined on the standard thermochemical scale. Symbols not including this denote quantities on the triple point scale.

The entropy, internal energy, and enthalpy can be treated by applying simple offset corrections along with adjustment of units using M_w (g mol^{-1}) the molecular weight of water. The requisite relations can be written as

$$S° = M_w\left[\left(s - s_{triple}\right) + k_s\right] \qquad (A-1)$$

$$\Delta_f U° = M_w\left[\left(u - u_{triple}\right) + k_u\right] \qquad (A-2)$$

$$\Delta_f H° = M_w\left[\left(h - h_{triple}\right) + k_h\right] \qquad (A-3)$$

Here k_s, k_u, and k_h are the respective offsets for the specific entropy, specific internal energy, and specific enthalpy (k_s was introduced in the main text). Recall that u_{triple} and s_{triple} are zero by convention. Recall also that $h_{triple} = P_{triple} v_{triple}$. Although this is small, it is not zero.

For the Helmholtz and Gibbs energies, there are two offsets for each. One is associated with the entropy. This can be thought of as the "slope" correction, as it affects the temperature dependence of both energy functions. The other can be thought of as the "intercept" correction (addition of a constant). The requisite standard thermodynamic relations are $a = u - Ts$ and $g = h - Ts$. Applying the slope correction first, one would redefine the specific Helmholtz energy as $a = u - T(s + k_s)$ and the specific Gibbs energy as $g = h - T(s + k_s)$. Then one would add an appropriate constant to each to complete the scale transformation. The resulting forms are

$$\Delta_f A° = M_w[u - T(s + k_s) + k_a] \qquad (A-4)$$

$$\Delta_f G° = M_w[h - T(s + k_s) + k_g] \qquad (A-5)$$

Here k_a and k_g are the respective intercept corrections.

Applying equations (A-1) through (A-5) to 298.15K and 1 bar and rearranging, one may obtain:

$$k_s = \frac{S^o_{298.15K,1\ bar}}{M_w} - \left(s_{298.15K,1\ bar} - s_{triple}\right) \qquad (A-6)$$

$$k_u = \frac{\Delta_f U^o_{298.15K,1\ bar}}{M_w} - \left(u_{298.15K,1\ bar} - u_{triple}\right) \qquad (A-7)$$

$$k_h = \frac{\Delta_f H^o_{298.15K,1\ bar}}{M_w} - \left(h_{298.15K,1\ bar} - h_{triple}\right) \qquad (A-8)$$

$$k_a = \frac{\Delta_f A^o_{298.15K,1\ bar}}{M_w} - u_{298.15K,1\ bar} + 298.15(s_{298.15K,1\ bar} + k_s) \qquad (A-9)$$

$$k_g = \frac{\Delta_f G^o_{298.15K,1\ bar}}{M_w} - h_{298.15K,1\ bar} + 298.15(s_{298.15K,1\ bar} + k_s) \qquad (A-10)$$

Table A-1 gives the constants calculated from the IAPWS-95 model and the CODATA (Cox et al., 1989) recommendations. Slightly different results would be obtained for other equation-of-state models.

Table A- 1. Simple offset constants for the IAPWS-95 model and the CODATA (Cox et al., 1989) thermochemical recommendations.

Constant	Value	Units
k_s	3.51562	kJ kg^{-1} K^{-1}
k_u	-15767.194	kJ kg^{-1}
k_h	-15970.895	kJ kg^{-1}
k_a	-11906.844	kJ kg^{-1}
k_g	-12110.528	kJ kg^{-1}

Appendix B. Notes on the Test Case Library

A library of test cases including examples of input files is included with the software. Each member of the test case library is designated by a unique three-part code of the form *abc*. Numbers may be used in place of letters. The main purpose of a test case is designated by a two-letter code of the form *AB*. A full designation therefore has the form *ABabc*.

There are three primary groups of test cases. Those beginning with "VC" are software verification test cases for which results are intended to be compared with mostly high-precision results given by other sources including IAPWS (2016). Those beginning with "TC" include some cases intended for comparison with results of others and some cases addressing performance evaluation. Those beginning with "MC" are more advanced test cases addressing the problem of multiple numerical solutions.

Some other group designators are used, mostly for groups with only one test case member. One test case beginning with "RC" (RCsar) is included for reference purposes. It calculates results for coexisting vapor and liquid at 298.15K, the thermochemical reference temperature. It is included because results for this temperature are not included in the steam tables of Wagner and Pruss (2002). One test case beginning with "PL" (PL640) is used to generate the blue curves shown in Figures 7-9 in Section 4.2.6.

Most members of the test case library are discussed in Sections 4 and 5 of this report. However, some test cases discussed in the report are not represented in the library. Conversely, some elements in the library do not correspond to cases discussed in this report. The input file for each test case contains a description of the purpose of the associated calculation.

Test case VCsct (discussed in Section 4.1.3) serves as an example of the structure of a test case included in the library. The relevant files are included in a folder named "VCsct". The relevant included files are:

input	the input file, ready to run (contains all problem input parameters)
input_sct	archival copy of the input file
output_sct	archival copy of the output file
out_sct	archival copy of the screen output
mtab_sct.csv	archival copy of the mtab.csv file
ctab_sct.csv	archival copy of the ctab.csv file
xtab_sct.csv	archival copy of the xtab.csv file

Running H2OI95 using the input file generates

output	the output file (text)
mtab.csv	the first .csv output file (comma-separated-variable)
ctab.csv	the second .csv output file (comma-separated-variable)
xtab.csv	the third .csv output file (comma-separated-variable)

If H2OI95 is run, specifying that the screen output be sent to a file called out ("H2OI95 > out", then the "out" file will also be produced.

The general idea is that output can be compared with output_sct, mtab.csv with mtab_sct.csv, and so on to verify that the code is operating correctly. This may be helpful if porting the software to a different platform, modifying the software, or for any reason recompiling it.

The batch files tch.bat and its associated batch files tchs.bat and tfcm1.bat act together (by running tch.bat) to run the entire test case library and compare copies of the output files with their corresponding archival files. The batch file tfcm1.bat requires a "sed" command, which is not a normal part of Microsoft Windows (it is common in Linux/UNIX). It is possible to find sed commands for Windows from various on-line sources.

Appendix C. Error in the Implementation of IAPWS-95 in H2OI95 Version 1.0

Section 5.2.1 of this report describes the implementation in H2OI95 Version 1.1 of the IAPWS-sanctioned model for the dynamic viscosity of water (IAWPS, 2008). In this model, the dimensionless viscosity $\overline{\mu}$ is represented by:

$$\overline{\mu} = \overline{\mu}_0(\overline{T}) \times \overline{\mu}_1(\overline{T}, \overline{\rho}) \times \overline{\mu}_2(\overline{T}, \overline{\rho})$$

where $\overline{T} = T/T_{cr} = 1/\tau$ and $\overline{\rho} = \rho/\rho_{cr} = \delta$. The third factor, $\overline{\mu}_2$, is called the critical enhancement. It is only necessary in a small region of density and temperature space around the critical point. This factor is a function of $\overline{T}$, $\overline{\rho}$, and the dimensionless isothermal compressibility ζ_T discussed in Section 5.1.3. Here ζ_T is calculated from the equation-of-state (EOS) model (IAPWS-95 or an alternative model such as IAPWS-IF97). Neither Wagner and Pruss (2002) nor IAPWS (2016) address this parameter, nor do they give information to use for computer verification of calculated values. The source documents describing the viscosity model (Huber et al., 2009; IAPWS (2008) give information for computer verification of viscosity values, but no direct information is provided for verification of ζ_T values, though one may properly infer that if values for the viscosity (or more specifically the critical enhancement) are correct, then the ζ_T values must also be correct.

IAPWS (2008) presents two tables for computer-program verification. The first is their Table 4, giving results obtained with $\overline{\mu}_2$ set to unity. This is intended to facilitate testing coding implementation of $\overline{\mu}_0$ and $\overline{\mu}_1$. As shown in Section 5.2.1 (Table 5.3), H2OI95 produced results matching the expected values to the precision given by IAPWS (2008).

The second of table from IAPWS (2008) (their Table 5, reproduced below) is for testing the coding implementation of the critical enhancement factor, $\overline{\mu}_2$. The temperature in all cases here is 647.35K, slightly above the critical temperature (647.096K). Comparison of results from H2OI95 (test case VCvis, second part) revealed significant discrepancies.

Table 5 from IAPWS (2008):

Table 5. Sample points for computer-program verification of the correlating equation, Eq. (10), in the region near the critical point.

T (K)	ρ (kg·m^{-3})	ξ (nm)	$\overline{\mu}_2$	μ (μPa·s)
647.35	122	0.309247	1.00000289*	25.520677
647.35	222	1.571405	1.00375120	31.337589
647.35	272	5.266522	1.03416789	36.228143
647.35	322	16.590209	1.09190440	42.961579
647.35	372	5.603768	1.03665871	45.688204
647.35	422	1.876244	1.00596332	49.436256

* Correlation length $\xi < 0.3817016416$ nm so Y is evaluated with Eq. (15).

The discrepancy was most prominent in the case for which the density is 322 kg-m^3, which is the critical density. This case presents the greatest values of correlation length (ξ) and critical enhancement. For this case, H2OI95 calculated a zero correlation length and a unit value for the critical enhancement.

A search for the source of the discrepancy led to an on-line viscosity calculator (http://twt.mpei.ac.ru/mcs/worksheets/iapws/wspsDVRT.xmcd) at the Moscow Power Engineering Institute (MPEI) created by the Russian National Committee (RNC) of the IAPWS. This calculator gives intermediate results in the calculation of the dynamic viscosity. The reported value of ζ_T for a density of 322 kg-m^3 was 831.6085703, whereas the value calculated by H2OI95 is a small number close to zero by comparison (see Table 5.4). Differences were smaller for the other density values in IAPWS (2008) Table 5. Hardwiring the RNC ζ_T values into H2OI95 gave results matching IAPWS (2008) Table 5, indicating that the problem in obtaining the expected values for the critical enhancement lay with the ζ_T values.

A re-examination of the relevant coding in H2OI95 revealed a coding error associated with the EOS model's 55th and 56th terms, which are more complex than any of the other terms. These terms are calculated in several pieces. The pieces were coded correctly, but the results were incorrectly assembled in subroutine EVAI95. Certain pieces were assembled in variables WW, WWd, and WWdd, and thence into corresponding variables HH, HHd, and HHdd, which were to be used in evaluating phi functions ϕ^r, ϕ^r_δ, and $\phi^r_{\delta\delta}$. Unfortunately, WW, WWd, and WWdd were used in place of HH, HHd, and HHdd in evaluating the relevant phi functions.

Table C.1shows ζ_T values for the IAPWS (2008) Table 5 cases, comparing results obtained from the uncorrected H2OI95, the MPEI RNC IAPWS-95 calculator, and the corrected H2OI95 (Version 1.1).

Results for the corrected H2OI95 are identical to the RNC IAPWS results to the number of significant figures shown.

Table C.1. Values of ζ_T for IAPWS (2008, Table 5) cases for computer-program verification in the region near the critical point. The temperature in all cases is 647.35K.

ρ (kg-m^{-3})	H2OI95 (version 1.0)	MPEI RNC Calculator*	H2OI95 (Version 1.1)
122	1.17236434	1.172359573	1.172359573
222	12.13628693	12.02261748	12.02261748
272	85.0003849	103.3499714	103.3499714
322	0.00000096**	831.6085703	831.6085703
372	56.57653032	85.37241366	85.37241366
422	9.25066217	8.93479199	8.934791993

*MPEI RNC IAWPS-95 on-line viscosity calculator:
http://twt.mpei.ac.ru/mcs/worksheets/iapws/wspsDVRT.xmcd.
**This value is effectively zero. It is obtained by resetting δ to a value just slightly different from unity in order to avoid a calculational singularity (see text).

For a density of 322 kg-m^{-3}, the IAPWS-95 model presents a numerical singularity [division by the quantity (δ - 1) when δ = 1] in the equation for the phi function $\phi_{\delta\delta}^{r}$, which is required to calculate $(\partial p/\partial\delta)_T$. That in turn is needed to obtain κ_T and ζ_T. The singularity is avoided by resetting δ to a value just slightly different from unity, such as 100 times the machine epsilon. The machine epsilon for 64-bit arithmetic on a Windows PC is about 2.2204 x 10^{-16}, hence 100 times that is about 2.2204 x 10^{-14}.

H2OI95 (Version 1.0) passed a significant number of verification tests, including all of the tests recommended by Wagner and Pruss (2002) and IAPWS (2016). . It is clear from the above findings that those tests are not completely sufficient to test the implementation of IAPWS-95. It is also necessary to test calculated values of ζ_T (and perhaps other "parameters) in a region close to the critical point.

In discussing the less than entirely satisfactory behavior of IAPWS-95 near the critical point, Wagner and Pruss (2002) reference a paper by Kiselev and Friend (1999). Those authors present an alternative EOS model and a possible modification to IAPWS-95 to obtain improved results near the critical point. Wagner and Pruss (2002) chose not to implement that modification in their model due to its additional complexity. However, Kiselev and Friend (1999) present plots of heat capacity functions close to the critical point. These plots address IAPWS-95, their proposed modification, and their own EOS model. These plots are useful in providing additional verification of the proper implementation of IAPWS-95 in H2OI95, although the comparisons are only graphical.

Figure 7(b) of Kiselev and Friend (1999) shows the isochoric heat capacity (c_v) at 647.1K as a function of density. The plot shown below (Figure C.1), obtained using H2OI95 (corrected), closely recreates the IAPWS-95 curve from that figure from Kiselev and Friend (1999). The uncorrected H2OI95 produced the identical curve.

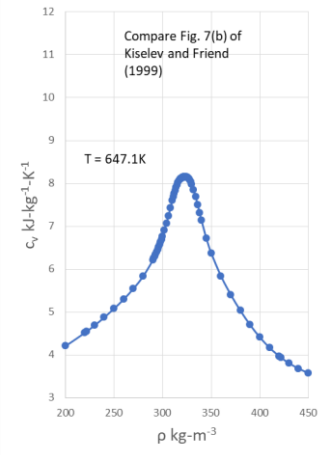

Figure C.1. Re-creation of Kiselev and Friend (1999) Figure 7(b) IAPWS-95 result using the corrected H2OI95.

Figure 8 of Kiselev and Friend (1999) shows the isobaric heat capacity (c_p) at 647.5K as a function of density. The corresponding result obtained using H2OI95 (corrected) is shown below in Figure C.2. This closely recreates the IAPWS-95 curve from Figure 8 of Kiselev and Friend (1999).

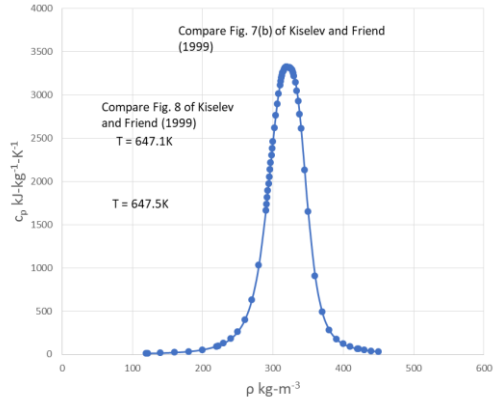

Figure C.2. Re-creation of Kiselev and Friend (1999) Figure 8 IAPWS-95 result using the corrected H2OI95.

Wagner and Pruss (2002) give similar plots in their Figures 6.11 and 6.12. Those plots could also be used for graphical verification near the critical point.

The nature of the code correction is further illustrated by comparing ζ_T as a function of δ at 647.35K, as calculated by the uncorrected and corrected code. Figure C.3 (left) shows the result obtained from the uncorrected code. Figure C.3 (right) shows the result obtained from the corrected code. The curve in the corrected case gives the expected value of 831.6085703 at δ = 1 (density of 322 kg-m^{-3}).

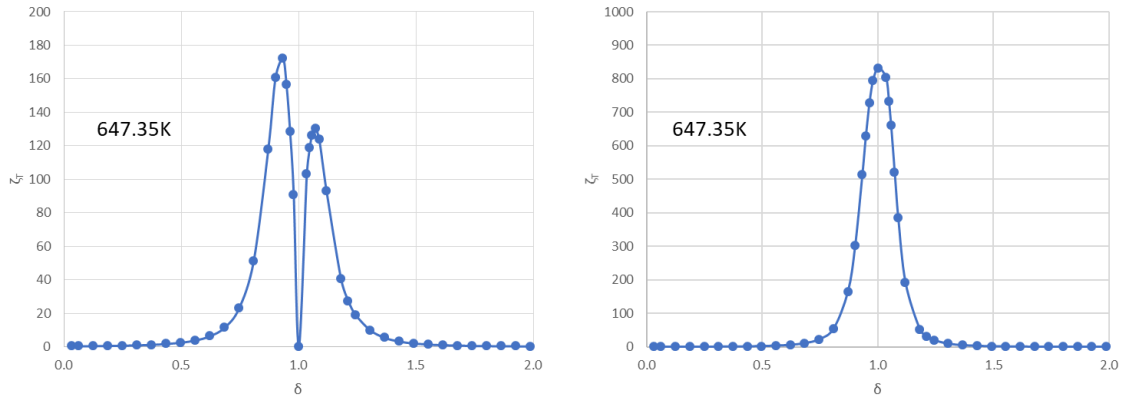

Figure C.3. ζ_T as a function of δ at 647.35K, calculated using the uncorrected H2OI95 (left) and the corrected H2OI95 (right). Note the change in scale (5x) on the vertical axis in the corrected case (right).

Values of ζ_T around the critical point cover a wide range, as this property approaches infinity at the critical point, as illustrated in Figure C.4 (left). Here the temperature is the critical temperature, 647.096K and the scaled density is varied about its critical point value of unity. The isothermal compressibility κ_T (Figure C.4, right) behaves similarly.

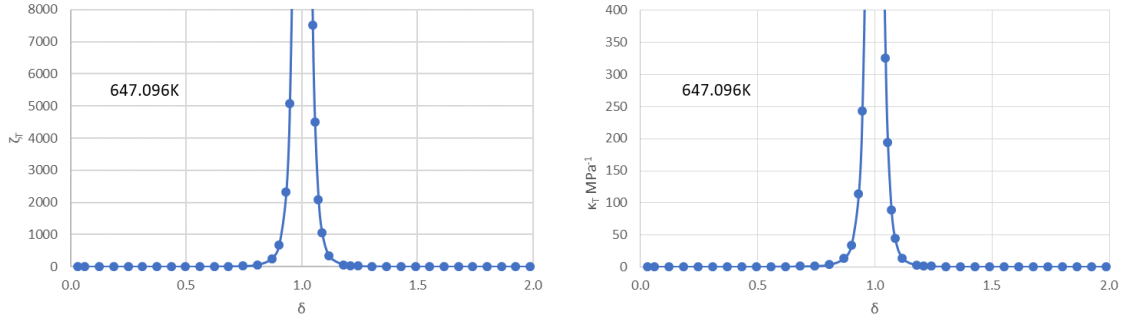

Figure C.4. Dimensionless compressibility ζ_T (left) and pressure (right) as functions of δ at 647.096K.

The implementation of the IAPWS (2008) viscosity model was helpful in uncovering a coding error in H2OI95. The coding error seems to be mainly consequential to "higher-order" functions such as c_p, κ_T, and ζ_T (which depend more strongly on the higher-order phi functions), with largest calculated errors near

the critical point. A substantial number of verification test cases ("VC" series tests) had been used in testing H2OI95 version 1.0, and they did not reveal problems. In other test problems, small differences from previous results were apparent near the critical point, as might be expected. In tests involving convergence ranges for starting values, the range boundaries changed in some cases. In cases not involving specified density, convergence was somewhat faster, due to the more accurate pressure derivative being supplied to the Newton-Raphson algorithm. Previous testing was "fortunate" in that it avoided stepping into the situation illustrated in Figure C.3, even though several convergence testing problems addressed points close to the critical point.

The verification test case given by IAPWS (2016) as Table 6 addresses phi functions for 500K and density of 838.025 kg m^{-3}. The corrected code gives the same results as before, exactly matching the test values. This test case is taken from Wagner and Pruss (2002, Table 6.6), who included a like test for 647K and density of 358 kg m^{-3}. The corrected code exactly produces the desired test values for this second case, whereas the uncorrected code produced slightly different values. At the time of initial verification of H2OI95, it was thought that the second part of this test case might have been dropped by IAPWS (2016) due to some issue with the test values given by Wagner and Pruss (2002). IAPWS (2016) did not explain why it did not include the second part of the original verification test case.

IAPWS (2011) describes the IAPWS-sanctioned model for the thermal conductivity of water. The model is developed in the corresponding paper by Huber et al. (2012). This model and its implementation are discussed in Section 5.2.2. The mathematical form of the thermal conductivity model follows (somewhat) that of the viscosity model described above. The dimensionless thermal conductivity $\overline{\lambda}$ is represented by:

$$\overline{\lambda} = \overline{\lambda}_0(\overline{T}) \times \overline{\lambda}_1(\overline{T}, \overline{\rho}) + \overline{\lambda}_2(\overline{T}, \overline{\rho})$$

where $\overline{T} = T/T_{cr} = 1/\tau$ and $\overline{\rho} = \rho/\rho_{cr} = \delta$. The third factor, $\overline{\lambda}_2$, is the critical enhancement, analogous to that for the viscosity. However, the critical enhancement here is a term *added* to $\overline{\lambda}_0 \times \overline{\lambda}_1$, not an additional factor to be multiplied by them.

The critical enhancement for thermal conductivity, like that for viscosity, also depends on the dimensionless isothermal compressibility ζ_T. Thus, if the thermal conductivity model had been implemented before that for the viscosity, the coding error described above would have been discovered when testing the thermal conductivity model.